

OPTICAL GLUCOSE NANOBIOSENSOR
ENCAPSULATING IN ERYTHROCYTES

A Dissertation
Presented to
the Faculty of the Graduate School
at the University of Missouri-Columbia

In Partial Fulfillment
Of the requirements for the Degree
Doctoral of Philosophy

By
MAJED EL-DWEIK
Dr. Sheila A. Grant, Dissertation Supervisor

MAY 2007

The undersigned, appointed by the Dean of the Graduate School,
have examined the dissertation entitled.

OPTICAL GLUCOSE NANOBIOSENSOR
ENCAPSULATING IN ERYTHROCYTES

Presented by Majed El-Dweik

a candidate for the degree of Doctor of Philosophy of Biological Engineering
and hereby certify that in their opinion it is worthy of acceptance.

Dr. Sheila A. Grant, Department of Biological Engineering

Dr. Mark Milanick, Department of Medical Pharmacology & Physiology

Dr. Mark Haidekker, Department of Biological Engineering

Dr. Charles E. Wiedmeyer, Department of veterinary Pathobiology

Dr. Xudong Fan, Department of Biological Engineering

Dedicated to my Lord the almighty Allah then to
my parents, wife and children

ACKNOWLEDGEMENTS

All Praise is due to the almighty God; the most Gracious and the most Merciful.

I would like to express my deepest gratitude to my advisor, Dr. Sheila Grant, for her advice, guidance, and encouragement throughout my Ph.D. program.

I would like to acknowledge all the members of my Ph.D. committee, Dr. Charles Wiedmeyer, Dr. Xudong (Sherman) Fan, Dr. Mark A. Haidekker, and Dr. Mark Milanick for reading the dissertation and for their constructive remarks.

I would like to thank Dr. David Emmerich at the University of Missouri-Columbia, for their advice and their useful suggestions.

Also, I extend my gratitude to the entire staff of the Department of Biological Engineering at the University of Missouri-Columbia. The technical support of our laboratory crew, Darcy Lichlyter, senior lab assistance, David Grant, and Krista Arnett from the Dr. Milanick laboratory during my experiments is highly appreciated.

I would like to express my special and deepest gratitude to my parents who supported me towards the success.

Last but not least, I would like to thank my dear wife, Cathy, for her patience, support, sacrifices, and encouragement during the years of my study.

Also, I'd like to express my love for my two children, Sarah and Ferris,
who give me the smile and hope for the whole life.

TABLE OF CONTENTS

ACKNOWLEDGEMENTS	-----	ii
LIST OF TABLES	-----	vii
LIST OF ILLUSTRATIONS	-----	vii
ABSTRACT	-----	xi

Chapter

1. LITERATURE REVIEW	-----	1
1.1 Introduction to Sensors and Biosensors	-----	1
1.1.1 Sensors and Biosensors	-----	1
1.1.2 Sensor Components	-----	2
1.1.2 Optical Transducer	-----	10
1.2 Optical Glucose Nanobiosensor Encapsulated in Erythrocytes	-----	22
1.2.1 Sensor Components	-----	22
1.2.2 Detection Equipments	-----	24
2. INTRODUCTION	-----	29
2.1 Background	-----	29
2.2 Significance	-----	31
2.3 Objectives	-----	33
3. NANOPROBES DEVELOPMENT	-----	35

3.1	Optical Glucose Nanoprobes Development -----	35
3.1.1	Introduction -----	35
3.1.2	FRET Method of Detection -----	36
3.1.3	Streptavidin and Biotin as Biological Markers --	36
3.1.4	Chosen FRET Fluorophore -----	38
3.1.5	Chosen Competitive Binding Markers -----	41
3.2	Materials and Methods -----	44
3.3	Results and Discussion -----	50
3.3.1	Fluorescence Resonance Energy Transfer (FRET) Experiments -----	50
3.3.2	Results of Dextran Size Effect on Glucose Response -----	51
3.3.3	Results of the Transmission Studies of FRET Glucose Sensors through Porcine Skin -----	57
3.4	Conclusions -----	60
4.	NOVEL GLUCOSE NANOPROBES -----	62
4.1	Glucose Binding Protein as a Novel Optical Glucose Nanobiosensor -----	62
4.1.1	Introduction -----	62
4.1.2	Materials and Method -----	65
4.1.3	Results and Discussion -----	68
4.1.4	Conclusions -----	76
5.	NANOPROBES ENCAPSULATION IN ERYTHROCYTES ---	77
5.0	Encapsulation of Streptavidin Labeled with Alexa Fluor 750 in Erythrocytes -----	77
5.1.1	Introduction -----	77
5.1.2	Materials and Method -----	80
5.1.3	Results and Discussion -----	82
5.2	Encapsulation of Streptavidin labeled with Alexa Fluor 680 and BSA labeled with Alexa Fluor 750 into Erythrocytes --	84
5.2.1	Method -----	84
5.2.2	Results and Discussion -----	85
5.3	Signal Detection of NIR Fluorescent Encapsulated Erythrocytes through Tissue -----	89
5.3.1	Method -----	89
5.3.2	Results and Discussion -----	89
5.3.3	Conclusions -----	92

6. SUMMARY AND FUTURE WORK	-----	94
REFERENCES	-----	98
VITA	-----	109

LIST OF TABLES

Table		Page
1.1	Properties of an ideal fluorophore and FRET pair	----- 21

LIST OF ILLUSTRATIONS

Figure	Page
1. Illustration of biosensor schematic layout -----	2
2. Jablonski diagram -----	12
3. Absorption and fluorescence emission spectra of perylene and quinine. -----	14
4. Schematic of FRET spectral overlap integral -----	17
5. Dependence of the energy transfer efficiency (E) on distance -----	19
6. Schematic diagram of a spectrofluorometer -----	25
7. Schematic of a PMT -----	27
8. Structure of Streptavidin -----	37
9. Streptavidin biotin-binding protein binding -----	38
10. Emission spectrum of AF 750 and Cy7 -----	39
11. Emission and Absorption spectrum of AF 680 and Cy5.5 -----	40
12. Scan of SA-AF 680 without the presence of BSA Biotin-AF 750 -----	50
13. Scan of SA-AF 680 with the presence of	

	BSA Biotin-AF 750 -----	51
14.	Glucose Response of AF680-dextran (10,000MW) and AF750-Con A -----	53
15.	Glucose Response of AF680-dextran (3000MW) and AF750-Con A -----	54
16.	Graph for determining the exponential function -----	55
17.	Glucose Response of AF680-dextran (3000MW) and AF750-Con A with larger detection limits-----	56
18.	Peak Signal from two different probes with tissue and without tissue -----	57
19.	The signal from different tissue thicknesses -----	58
20.	Relation between tissue thickness and intensity -----	59
21.	Schematic of the geometry of the glucose-binding sites -----	63
22.	Background signal of AF750 on cysteine before the labeling with AF680 and after -----	69
23.	Donor peaks at 702 nm with and without acceptor presence ----	70
24.	D/A vs. glucose concentration (detection range 0 to 120uM) --	72
25.	D/A vs. glucose concentration (detection range 0 to 60uM) ----	73
26.	Glucose response to different samples at t=0min. -----	74
27.	Average glucose response to different samples at t=0min. ---	73
28.	Glucose response of three samples at t=0min. -----	74
29.	Glucose response to different samples at t=5min. -----	75
30.	An SEM image of red blood cell. The cells were obtained from rabbits -----	77
31.	Biotechnol. Appl. Biochem. (1998) 28, 1–6 -----	78
32.	Loaded red cell overall design -----	79

33.	Fluorescence signal acquisition of AF750 dye loaded into red cells	-----	83
34.	Scan of supernatant sample 1	-----	85
35.	Scan of loaded cells sample 1	-----	86
36.	Scans of supernatant and loaded cells sample 2	-----	87
37.	Scan of supernatant sample 3	-----	88
38.	Scan of the loaded cells sample 3	-----	88
39.	Set up of the tissue wrapped	-----	90
40.	Fluorescence signal capture of AF750 dye through a porcine aorta.	-----	92

OPTICAL GLUCOSE NANOBIOSENSOR ENCAPSULATED IN ERYTHROCYTES

Majed El-Dweik

Dr. Sheila Grant, Dissertation Supervisor

ABSTRACT

Optical nanobiosensor encapsulated in erythrocytes, Red Blood Cells (RBC's), is a novel nanotechnology. This nanotechnology will be utilized for In Vivo detection such as glucose concentration in blood. The determination of blood glucose concentration is very important in diabetics. By developing a continuous implantable detection system, diabetics will have freedom from the manual painful testing and also error free testing.

Diabetes has become a wide spread disease not only among adults but also among children. In 2005 the American Diabetes Association (ADA) reported that 20.8 million people have diabetes, making it the fifth leading cause of death by disease in the U.S and also contributing to higher rates of morbidity. People with diabetes are at higher risk for heart disease, blindness, kidney failure, extremity amputations, and other chronic conditions. In 2002, the ADA reported direct medical and indirect expenditures attributable to diabetes were estimated at \$132 billion. In July 2005 ADA reported about a new type of diabetes called

slow-onset diabetes or diabetes 1.5, which has similarities both to type 1 and type 2. It is recognized as type 1.5, because at first, it looks like and reacts positively to treatments for type 2. However, it ends up revealing itself as an autoimmune form of diabetes, more like type 1.

Diabetics must closely monitor their glucose levels in order to avoid the detrimental effects of the disease. The available glucose meter requires patients to prick their finger (up to 7 times a day) and place a drop of blood on a test strip to determine blood glucose concentration. To prevent patient from going through this painful process one has to develop an ideal implantable glucose sensor that could be interfaced with an implantable insulin pump would provide a closed loop for an automatic control of glucose levels.

Successful implementation of nanotechnology will help in improving glucose monitoring and management. The innovation of nanocellular glucose biosensor arises, not only from the fluorescent probes, but also from the insertion of the nanoprobe into RBCs.

Recently, increase focus has been placed upon the development of sensors and biosensor devices for the long-term monitoring and managing of health conditions. In particular, glucose sensors have been heavily investigated. The main objective in these investigations has been to develop an ideal sensor with ultra-sensitivity, high selectivity, reliability, limited biofouling, and low cost. While those features could be found in some of the developed implantable sensors, biofouling imposed a major problem.

Implantable sensors suffer from biofouling. Biofouling is caused by nonspecific adsorption of proteinaceous materials to the sensor surface. This material will encapsulate the implantable device and render it inoperable. The encapsulation accrues few days later where the fibroblasts cells migrate to the implant surface and contribute to the encapsulation process through proliferation then surrounding the implant to isolate from the body. The result from the above effects is isolation of the sensing surface from the analyte, which lead to delay, or inaccurate measurements.

There are several techniques for improving biocompatibility and thus reducing biofouling. One of which is a polymeric material as membrane coatings to modify the surface charge and wettability of the sensor substrate. However, long-term biocompatibility was still a problem.

To overcome biocompatibility problems, RBCs will be utilized to isolate the biosensor and result in fast response to glucose concentration.

While RBCs have been utilized as carrier for therapeutic agents, they have not been used as carriers for glucose sensors. RBCs have potential advantages for use as a glucose sensor carrier. RBCs can transport glucose in and out of the cell for most species, and this transport is insulin independent. Also the Hypo-Osmotic dialysis technique can quickly load a significant number of RBCs with probes resulting in a 93% survival rate and a normal mean cell life and cell half-life. Another advantage of RBCs, they have no organelles including neither nuclei nor ribosome, thus RBCs can not synthesize new proteins and

thus are designed to provide a milieu where enzymes remain functional for 120 days.

There are many fluorescent probes that monitor glucose accurately. Concanavalin A and Dextran were labeled with acceptor and donor dyes respectively. In the presence of glucose, the labeled Dextran was displaced from the Concanavalin A resulting in a change in fluorescence. The sensors are being placed in microspheres, which have yet to be investigated for biocompatibility and to ensure that the toxic Concanavalin A does not leach out of the microspheres.

The merger of two techniques: Fluorescence Resonance Energy Transfer (FRET) competitive binding method and hypo-osmotic dialysis of RBCs in order to develop a novel RBC/nanoprobe glucose sensor. This technique offers the advantages of reducing sensor incompatibility by utilizing RBCs as protective, biocompatible carrier. Another advantage is stable, specific response to glucose through the utilization of FRET nanoprobes and avoiding the need for nanospheres, which can suffer fabrication uniformity and leaching. Also long-term sensor is more convenient and less invasive than current sensors used.

An implantable glucose biosensor encapsulated in RBCs will become a method for continuously measuring blood glucose concentration in diabetics. The nanoprobes will be constructed by using competitive binding technique between glucose binding enzyme (GBE) and dextran. Then both of them will be labeled with FRET dye pair such as Alexa Fluor 750 and Alexa Fluor 680 respectively.

Using a procedure modified from the Molecular Probes labeling kits. The donor and acceptor will be encapsulated in RBCs. Dextran binds to a GBE, but in the presence of glucose, the donor-dextran gets displaced from the acceptor-GBE, resulting in changing in acceptor fluorescence and in donor fluorescence as the glucose binds with the GBE. Fluorescence spectra confirmed this result.

Glucose Binding Protein (GBP) is another protein that binds with high affinity to glucose. GBP is a monomeric periplasmic protein. It is synthesized in the cytoplasm of *Escherichia coli* which functions as a receptor for transport D-glucose. The binding mechanism is based on a hinge motion due to the protein conformational change. This change could be used as an optical sensing mechanism by applying a FRET system. The wild-type GBP lacks cysteine in its structure, but by introducing a single cysteine at a specific site by site-directed mutagenesis, this will ensure single-label attachment at specific sites with a fluorescent probe. Site-directed mutagenesis by overlap extension PCR was performed to prepare a mutant to introduce a single cysteine residue at positions 175. The other sites are amino sites, which will be labeled with another fluorophore. NIR FRET pair, Alexa Fluor 680 (AF680) and Alexa Fluor 750 (AF750), was used. The AF680 will target the ammine sites, which become the donor. The AF750 will label the single cysteine site, which becomes the acceptor. Since this residue is not involved in ligand binding and since it is located at the edge of the binding cleft, it experiences a significant change in environment upon binding of glucose. The sensing system strategy is based on the fluorescence changes of the probe as the protein undergoes a structural change on binding.

This nanobiosensor has the ability to detect submicromolar, 25uM concentrations of glucose. These results will be used as a potential technique to detect deferent glucose concentrations in blood.

CHAPTER 1

LITERATURE REVIEW

1.1 Introduction to Sensors and Biosensors

1.1.1 Sensors and Biosensors

A sensor is a device that detects or measures physical properties. It can also record, indicate, or respond to physical properties. There are three types of sensors.

- a. Physical sensors, which can measure physical quantities such as length, weight, temperature, pressure, and electricity.
- b. Chemical sensors, which can respond to a particular analyte in a selective way through a chemical reaction and can be used for the qualitative or quantitative determination of the analyte's properties. Chemical sensors could detect and measure a specific chemical substance or set of chemicals.
- c. Biosensors are devices that utilize a biological sensing element connected to a transducer. Biosensors could detect and measure purely chemical [1].

This project is based on a biosensor principle. The first biosensor was designed in 1963 using an electrochemical electrode. Biosensors are analytical devices incorporating a biological or biologically derived material intimately associated with or integrated within a physico-chemical transducer or transducing

microsystem. They can be optical, electrochemical, thermometric, piezoelectric or magnetic.

Biosensors can provide rapid measurement of alcohol in wines, biogenic amines as indicators of food freshness, lactulose as indicator of milk quality or the presence of contaminants such as pesticides, toxins and microbes for instance.

1.1.2 Sensor components

Sensors consist of the following components (Figure 1.1);

- a. A recognition element, which is selective to certain analyte (substrate).
- b. A transducer is where a signal will be extracted.
- c. A signal processing device, which will analyze a detected signal.

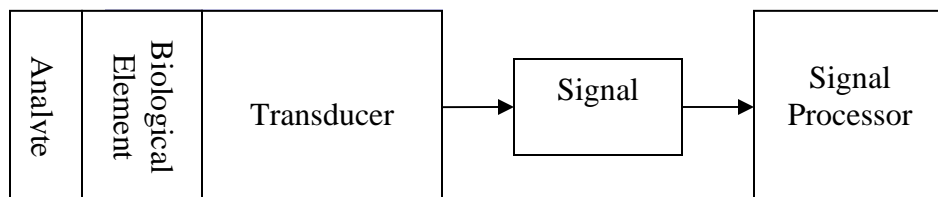


Figure 1.1. Illustration of biosensor schematic layout

Recognition Elements

Recognition elements enable a sensor to respond selectively to a particular analyte or group of analytes. Also they avoid interferences from other substances. The analysis method for specific ions has been to use ion-selective electrodes, which usually contain a membrane selective for the analyte of choice.

The most common recognition elements in biosensors are enzyme, antibodies, nucleic acids and receptors.

Transducers

Most sensors are known to have electrochemical transducers, because they are easy to construction and inexpensive. The development of photon-driven devices through the use of optical fibers will eventually compete with electrical appliances such as telephone lines. In addition, the use of micro-mass-controlled devices, based mainly on piezo-electric crystals, may become competitive in the near future.

Transducers can be subdivided into four main types, electrochemical, optical, piezo electric, and thermal.

1. Electrochemical Transducers

(i) *Potentiometric.*

Potentiometric involves the measurement of the potential (emf) of a cell at zero current. The emf is proportional to the logarithm of the concentration of the substance being determined.

(ii) *Voltametric.*

Voltametric measurement is the increasing or the decreasing potential when it is applied to the cell until oxidation or reduction of the substance to be analyzed occurs. There is a sharp rise or fall in the current to give a peak current. If the appropriate oxidation or reduction potential is known, one may step the potential directly to that value and observe the current. This mode is known as *amperometric*.

(iii) *Conductometric.*

Conductometric measurement is the change in the electrical conductivity of the solution, which is a result from most reactions that involve a change in the composition of the solution. That can be measured electrically.

(iv) *Field-Effect-Transistor-based sensors.*

Field-Effect-Transistor-based sensors are miniaturized type of electrochemical transducers on a siliconchip- based field-effect transistor. This is used with potentiometric sensors, but it could be used with voltametric or conductometric sensors.

2. Optical Transducers

Fiber optic sensor is an example of optical transducers. This development is allowing greater flexibility and miniaturization. These techniques are used in absorption spectroscopy, fluorescence spectroscopy, luminescence spectroscopy, internal reflection spectroscopy, surface plasmon spectroscopy and light scattering.

3. Piezo-electric Transducers

These devices are designated to generate electric currents from a vibrating crystal. The frequency of vibration is affected by the mass of material adsorbed on its surface, which could be related to changes in a reaction. Surface acoustic wave devices are a related system.

4. Thermal Sensors

Heat generated and produced from any reaction from any chemical or biochemical reaction can be measured by using sensitive thermistors.

Method of Immobilization

The recognition element and the transducer have to be connected in a sensor. This selective element can be connected to the transducer by using several methods. Those methods are adsorption, microencapsulation, entrapment, covalent attachment, and cross-link.

1. Adsorption

The simplest method is adsorption on to a surface.

2. Microencapsulation

Microencapsulation is the term used for trapping between membranes. It is one of the earliest methods to be employed.

3. Entrapment

Entrapment is where the selective element trapped in a matrix of a gel, paste or polymer. This is a very popular method.

4. Covalent attachment

Covalent attachment is where covalent chemical bonds formed between the selective component and the transducer.

5. Cross-linking

Cross-linking is where a bifunctional agent is used to bond chemically the transducer to the selective component. This is often used in conjunction with other methods, such as adsorption or microencapsulation.

Performance Factors

The performance factors of a sensor are imperative to the operation. These factors are the selectivity, sensitivity, accuracy, nature of solution, response time, and work lifetime.

1. Selectivity

Selectivity is the most important characteristic of sensors – the ability to discriminate between different substances. Such behavior is principally a function of the selective component, although sometimes the operation of the transducer contributes to the selectivity.

2. Sensitivity range

Sensitivity range usually needs to be sub-millimolar, but in special cases can go down to the femtomolar (10⁻¹⁵ M) range.

3. Accuracy

Accuracy needs to be better than $\pm 5\%$.

4. Nature of solution

Nature of solution conditions such as pH, temperature and ionic strength must be considered.

5. Response time

Response time is the amount of time the sensor response after being exposed to the analyte of interest. Typically, the response times are measured in the form of τ_{90} , the time necessary for 90% of the total response. Preferred response times should be less than 30 seconds. But response times are usually much longer (30 s or more) with biosensors than with chemical sensors.

6. Recovery time

Recovery time is the time that elapses before the sensor is ready to analyze the next sample. It must not be more than a few minutes.

7. Working lifetime

The working lifetime is usually determined by the stability of the selective material. For biological materials this can be as short as a few days, although it is often several months or more.

Area of Application

1. Health Care

Health care is the main area of application of biosensors and chemical sensors (*chemisensors*). Measurements of blood, gases, ions and metabolites are regularly needed to show a patient's metabolic state – especially for those in the hospital, and even more so if they are in intensive care. Many of these

substrates have been determined by samples of urine and blood being taken away to a medical analytical laboratory for classical analysis, which may not be completed for hours or even days. The use of point-of-care sensors and biosensors enable results to be obtained in minutes at most.

Point-of-care biosensors would obviate the need for *en suite* analytical units with specialist medical laboratory scientists. A trained nurse would be competent enough to carry out sensor tests at the bedside. Modern 'smart' sensors, based on field-effect transistors (FETs), may combine several measurements into one sensor unit. This particularly applies in the case of ion sensors for sodium, potassium, calcium and pH. Attempts are also being made to make combination or multi-analyte biosensors, e.g. for glucose, lactate and urea.

A potential 'dream application' is to have an implanted sensor for continuous monitoring of a metabolite. This might then be linked via a microprocessor to a controlled drug-delivery system (e.g. an iontophoretic system) through the skin. Such a device would be particularly attractive for chronic conditions such as diabetes. The blood glucose sensor would be monitored continuously and, as the glucose level reached a certain value, insulin would be released into the patient's blood stream automatically. This type of system is sometimes referred to as an *artificial pancreas*. The system would be far more beneficial for the patient than the present system of discrete blood glucose analyses which involves pricking the fingers every time, followed by injection of large doses of insulin every few hours.

2. Control of Industrial Processes

Sensors are used in various aspects of fermentation processes in three different ways, i.e. (i) off-line in a laboratory, (ii) off-line, but close to the operation site, and (iii) on-line in real time. At present, the main real-time monitoring is confined to such measurements as temperature and pH, plus carbon dioxide and oxygen measurements. However, biosensors that monitor a range of direct reactants and products are available, such as those for sugars, yeasts, malts, alcohols, phenolic compounds, and perhaps, undesirable by-products. Such monitoring could result in improved product quality, increased product yields, checks on tolerance of variations in quality of raw material, optimized energy efficiency, i.e. improved plant automation, and less reliance on human judgment. In general, there is a wide range of applications in the food and beverage industry.

3. Environmental Monitoring

There is an enormous range of potential analytes in air, water, soils, and other environmental situations. Such measurements in water include biochemical oxygen demand (BOD), acidity, salinity, nitrate, phosphate, calcium and fluoride. Pesticides, fertilizers and both industrial and domestic wastes require extensive analyses. Continuous real-time monitoring is required for some substances, and occasional random monitoring is needed for others. Pollution, farming, gardening, veterinary science and mining are all areas where sensors are needed for environmental monitoring.

1.1.3 Optical Transducer

Optical biosensors can be used to detect changes in concentration, mass, or number of molecules. Those changes can be related to changes in the characteristics of light. There are several techniques used such as absorption spectroscopy, fluorescence spectroscopy, luminescence spectroscopy, internal reflection spectroscopy, surface plasmon spectroscopy and light scattering.

1. Fluorescence

Fluorescence is considered as a primary technique to study molecular interactions in clinical chemistry, environmental monitoring, DNA sequencing, and genetic analysis as well as in the biological sciences [2]. The fluorescence technique has expanded to also include optical sensing.

There are several advantages to the utilization of fluorescence detection sensors. They are highly sensitive, operate at a high speed and relatively safe compared to other light-based investigation methods. Fluorescence is also considered as a non-invasive technique, which would not harm or destroy used sample in the process nor produce any hazardous byproducts. Sensitivity is another critical factor for designing a sensor. A fluorescence signal provides that sensitivity and is also proportional to the concentration of the substance that is investigated. Fluorescence detection can be used to determine distances within macromolecules to be measured, binding of biochemical species to be easily studied *in situ*, dynamics of the folding and unfolding of proteins to be studied and concentrations of ions to be measured inside living cells. Research on

membrane structure and function may also be performed with fluorescence probes. Additionally, drug interactions with cell receptors can be investigated, and minute traces of fluorescent materials can be detected and identified in mixtures.

Luminescence is divided into fluorescence and phosphorescence, and it is the emission of light from any substance and occurs from electronically excited states [2]. Fluorescence is the phenomenon by which absorption of light at a given wavelength by a fluorescent molecule is followed by the emission of light at longer wavelengths. Fluorescence typically occurs from aromatic molecules such as quinine, Fluorescein and rhodamine B. One widely encountered fluorophore is quinine, which is present in tonic water and it is excited by the UV light from the sun. The processes, which occur during the absorption and emission of light, are illustrated by a Jablonski diagram (Figure 1.2). The singlet ground, first and second electronic states are depicted by S_0 , S_1 , and S_2 , respectively.

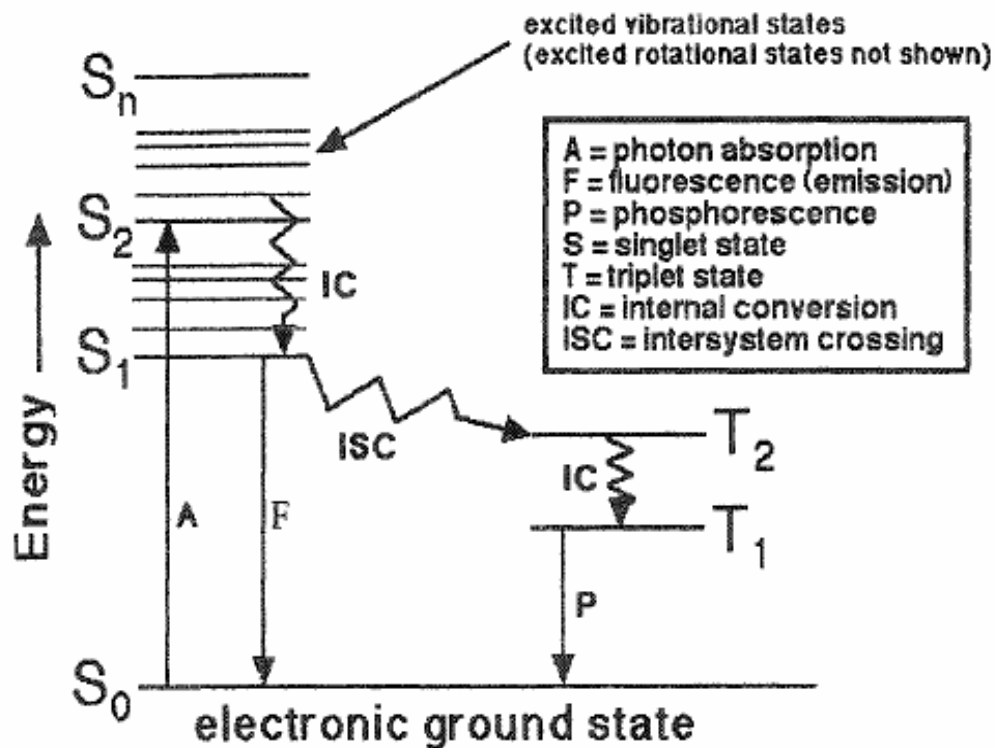


Figure 1.2. Jablonski diagram [3].

Absorption usually occurs from molecules at the lowest vibrational energy levels, S_0 . An electron in the fluorophore is typically excited to some higher vibrational level of either S_1 or S_2 and then relaxed to the lowest vibrational level of S_1 , via a process called internal conversion. This process is a radiationless transition between energy states of the same spin state, and generally occurs in 10^{-12} s or less. Fluorescence emission usually occurs from the lowest-energy vibrational state of S_1 to the ground electronic state of the same spin state.

Fluorophores containing heavy atoms in the S_1 state undergo a radiationless transition to the different spin state, T_1 , which is called intersystem crossing.

The emission from T_1 to S_0 is termed phosphorescence, as shown in Figure 1.2. The lifetimes of fluorescent states are very short from 10^{-5} to 10^{-8} s, compared to that of phosphorescence (10^{-4} seconds to minutes). Additionally, fluorescence is statistically much more likely to occur than phosphorescence.

Emission spectra depend on not only the chemical structure of the fluorescence molecules but also the solvent in which they are dissolved. The energy spacing between the various vibrational energy levels is demonstrated by the emission spectrum of perylene compared to quinine in Figure 1.3 [2]. The spectrum of perylene shows significant structure because of the individual vibrational energy levels of the ground state and excited states, whereas quinine shows spectrum devoid of vibration structure.

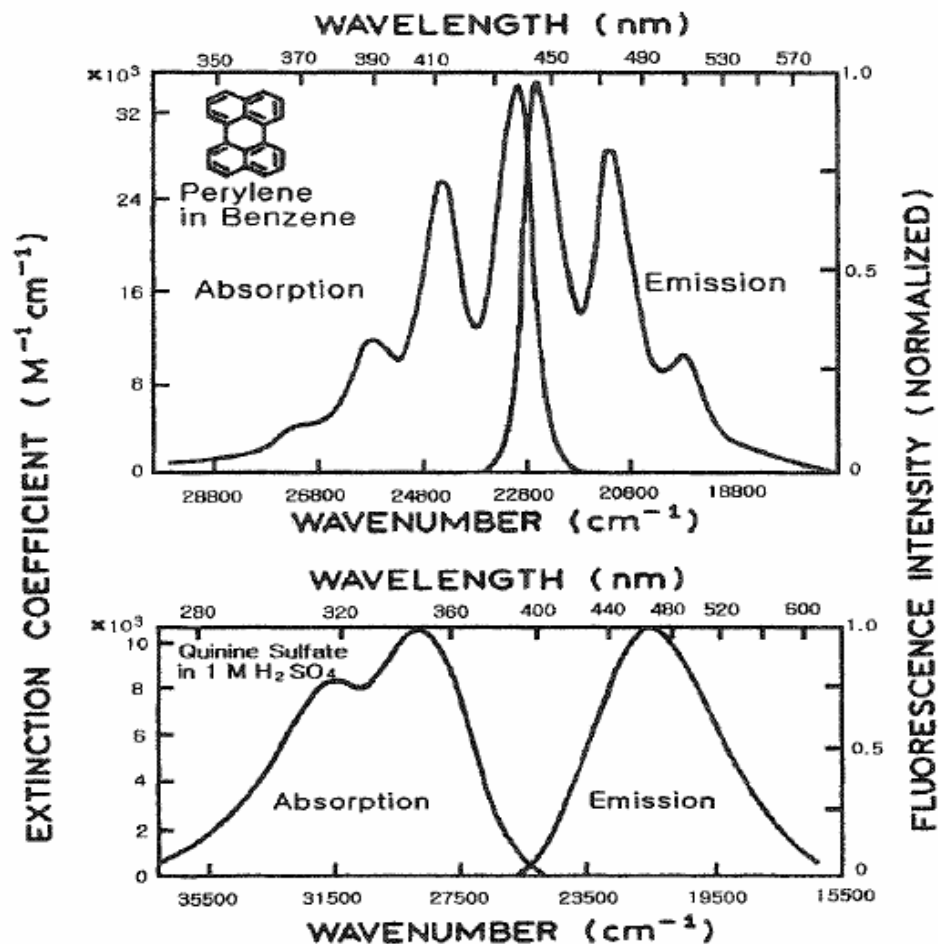


Figure 1.3 Absorption and fluorescence emission spectra of perylene and quinine. Emission spectra cannot be correctly presented on both the wavelength and the wave number scales. The wave number presentation is corrected in this instance. Wavelength is shown for convenience. [2]

Generally, fluorophores are divided into two classes, intrinsic and extrinsic. Intrinsic is naturally occurring fluorescence whereas extrinsic are usually organic dyes that are labeled to a sample mat does not show the desired spectral properties.

For fluorescence, the dominant fluorophore in proteins is the indole group of tryptophan, its absorption and emission wavelength is near 280 nm and 340 nm, respectively. Several biological molecules also display significant fluorescence. They include reduced nicotinamide adenine dinucleotide (NADH) and oxidized flavins adenine dinucleotide (FAD). For extrinsic fluorescence, Diphenyl hexatriene (DPH) is one of the most commonly used membranes probes. Membranes generally do not display intrinsic fluorescence, so DPH can be used to label membranes spontaneously partitioned into the nonpolar side-chain region. Two of the most widely used probes, dansyl chloride (DNS-C1) and fluorescein isothiocyanate (FITC), react with the free amino groups of proteins, allowing conjugation, which causes the proteins to fluoresce at the blue or green wavelengths, respectively.

The fluorescence lifetime (τ) and quantum yield (Q) are the most critical properties of a fluorophore. The fluorescence quantum yield is the ratio of photons emitted through fluorescence to photons absorbed. In other words, the quantum yield gives the probability of the excited state being deactivated by fluorescence rather than by another, non-radiative mechanism. Molecules with the largest quantum yields generate the brightest fluorescence. The fluorescence quantum yield, which is governed by the emissive rate of the fluorophore (Γ) and its rate of nonradiative decay to S_0 (K_{nr}), is given by equation 1.1:

$$Q = \frac{\Gamma}{\Gamma + K_{nr}} \quad (\text{eqn. 1.1})$$

The quantum yield can be close to unity when the nonradioactive decay rate is much smaller than the rate of radiative decay ($K_{nr} \ll \Gamma$). The quantum

The lifetime is the average time the molecules spends in the excited state prior to return to the ground state (S_0), and it determines the time available for the fluorophore to interact with its environment. Also, fluorescence lifetime indicates the time it takes for 63% of the population to emit. Fluorescence lifetimes are typically about 10 nanoseconds. The lifetime of fluorophore is illustrated by equation 1.2:

$$\tau = \Gamma (\Gamma + K_{nr}) \quad (\text{eqn. 1.2})$$

Quenching can reduce the intensity of fluorescence. The excited-state fluorophore is deactivated if it contacts other molecules, i.e., quenchers, in a solution. This phenomenon is called collisional quenching, which is illustrated by Stern-Volmer equation 1.3:

$$F_0/F = 1 + K[Q] = 1 + k_q \tau_0 [Q] \quad (\text{eqn. 1.3})$$

where K is the Stern-Volmer quenching constant, k_q is the bimolecular quenching constant, τ_0 is the unquenched lifetime, and $[Q]$ is the quencher concentration. The quenching occurs due to electron transfer from fluorophore to quencher, spin-orbit coupling, and intersystem crossing to the triplet state. Another quenching process is static quenching that occurs in the ground state.

Static quenching results in nonfluorescence complexes being formed with quenchers and fluorophores.

Fluorescence resonance energy transfer (FRET) is the transfer of the excited state energy from the initially excited donor fluorophore (D) to an acceptor fluorophore (A) [2], which is based on the distance between donor and acceptor fluorophores. The spectrum of donor molecules emitted must overlap the absorption spectrum of the acceptor molecules. When donor and acceptor molecules are in close proximity (less than 100 Å, known as the Forster distance) of each other, the excited state energy from the donor fluorophores can be transferred to the acceptor fluorophores nonradiatively not by emission of a photon but by dipole-dipole interactions between the donor and acceptor. This results in a reduction in the donor's fluorescence intensity and excited state lifetime, with a corresponding increase in the acceptor's emission intensity. The donor's fluorescent lifetime decreases with increasing FRET. A schematic of the FRET spectral overlap integral is shown in Figure 1.4.

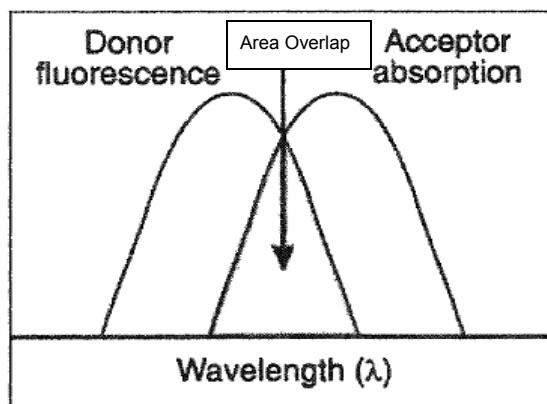


Figure 1.4 Schematic of FRET spectral overlap integral [2]

The efficiency of FRET strongly depends on the inverse sixth power of the two fluorophores separation distance, which makes it useful over distances comparable to the dimensions of biological macromolecules. The efficiency of energy transfer is determined as the fraction of photon energy absorbed by the donor that is transferred to the acceptor, which is the ratio of the transfer rate to the total decay rate of the donor. This fraction is given by equation 1.4:

$$E = \frac{k_T}{(1/\tau_D) + k_T} \quad (\text{eqn. 1.4})$$

where τ_D is the fluorescence lifetime of donor in the absence of an acceptor, k_T is the rate of energy transfer from a donor to acceptor and it is given by equation 1.5:

$$k_T = 1/\tau_D (R_0/r)^6 \quad (\text{eqn. 1.5})$$

where R_0 is the Forster distance (The distance at which FRET is 50% efficient, which ranges from 20 to 100 Å), r is the distance between donor and acceptor. The efficiency of energy transfer can be also be rearranged as the following equation 1.6:

$$E = R_0^6 / (R_0^6 + r^6) \quad (\text{eqn. 1.6})$$

This equation indicates that the transfer efficiency strongly depends on distance, when the distance between the donor and acceptor is near R_0 (Förster distance) (Figure 1.5).

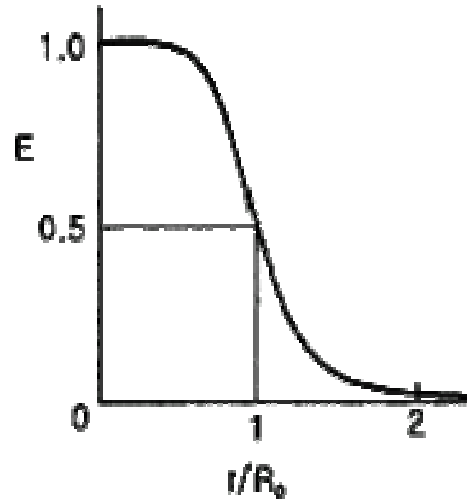


Figure 1.5. Dependence of the energy transfer efficiency (E) on distance. R_0 is the Förster distance. [2]

As the distance between two fluorophores decreases below R_0 , the transfer efficiency quickly increases while it quickly decreases to zero when r is greater than R_0 .

The transfer efficiency can also be shown using not only the relative fluorescence intensity of the donor in the presence (F_{DA}) and absence (F_D) of acceptor, but also the lifetime of the donor in the presence (F_{DA}) and absence (τ_D) of acceptor. They are given by the following equations 1.7 and 1.8:

$$E = 1 - (F_{DA}/F_D) \quad (\text{eqn. 1.7})$$

$$e = 1 - (T_{DA} / T_D) \quad (\text{eqn. 1.8})$$

These equations can be used to determine the transfer efficiency of the FRET pairs in the study and only useful to FRET pairs separated by a fixed distance.

Thus, FRET is one of the few tools that are able to measure nanometer scale changes in distance, both *in vitro* and *in vivo*. For instance, it can be used to measure the distance between sites on macromolecules and conformational changes of moving domains in the case of multidomain proteins.

2. Fluorophore/FRET pair

There is large selection of fluorophores provided by different companies. These fluorophores differ in their excitation, emission, quantum yield, and other properties. Since the FRET technique is utilized in this project, the chosen fluorophores must fulfill the FRET requirements discussed in the previous section. This project requires a fluorophore/FRET pair with special properties. Those ideal properties are listed in Table 1.

Table 1.1 Properties of an ideal fluorophore and FRET pair

Ideal Fluorophore/FRET pair
<ol style="list-style-type: none">1. high quantum yield2. non-toxicity3. longer emitting fluorophores4. large Stokes shift5. sharply spiked emission wavelengths6. long excited-state lifetime7. insensitive to pH8. photo-stability when conjugated9. strong energy transfer (FRET pair)10. easily to conjugate11. can be excited with commercially available laser diodes

The Alexa Fluor 680 and the Alexa Fluor 750

The donor, the Alexa Fluor 680, has an excitation and emission at 680 nm and 705 nm respectively. The long-wavelength the Alexa Fluor 680 exhibits bright red fluorescence that is easily distinguished. It is also a fixable, far-red-fluorescent tracer for long-term cell labeling. The succinimidyl ester (SE) reactive group forms a strong covalent attachment to primary amines that occur in proteins and other biomolecules inside of cells. With its far-red fluorescence, cell trace far red DDAO-SE has minimal spectral overlap with most other fluorophores and can be used with Alexa Fluor 750.

The acceptor, Alexa Fluor 750 excites and emits at 752 and 779 nm respectively. As the longest-wavelength Alexa Fluor dye, the emission is well separated from commonly used far-red fluorophores such as Alexa Fluor 647 dye or allophycocyanin (APC), facilitating multicolor analysis. Fluorescence of this long-wavelength Alexa Fluor dye is not visible to the human eye but is readily detected by most imaging systems.

This pair is advantageous because both fluorophores are biocompatible, have superior quantum yields, are insensitive to pH, and have lower background than conjugates of the other commonly used fluorescent dyes. They also have high chemical stability and very good resistance to photo bleaching.

1.2 Optical Glucose Nanobiosensor Encapsulated in Erythrocytes

1.2.1 Biosensor Components

The target of this project is to design a biosensor to sense glucose in the blood continuously. Therefore a biosensor design has to include all required components such as a recognition element, a transducer and signal processing device.

An Enzymatic Biological Recognition Element

Enzymes are protein biocatalysts. Each enzyme can act on a specific substrate. There are several types of enzymes. The most common ones are enzymes that catalyze the oxidation of compounds using oxygen or NAD and the

hydrolases catalyzing the hydrolysis of compounds [4]. Glucose oxidase (GOx) was used as a biological sensing element to catalyze oxidation of glucose for the development of a biosensor [5]. There are several advantages of using enzymes in sensors. They are considered as highly selective, fairly fast-acting, and sensitive when used as recognition elements. Hexokinase is another enzyme that has high affinity to glucose [6].

There have been several reported designs for enzymatic glucose nanoprobe. Some of the designs utilize Fluorescence Resonance Energy Transfer (FRET) competitive binding, which include a GOx/dextran nanoprobe, glucose dehydrogenous (GDH)/dextran nanoprobe, and a Concanavalin A (Con A)/dextran nanoprobe. Another nanoprobe that has been reported utilizes conformational changes upon glucose binding to elicit changes in FRET. This nanoprobe design includes FRET labeled bacterial glucose-binding protein (GBP).

There are many fluorescent probes that monitor glucose accurately. For example, a series of experiments were performed using FRET competitive binding technique. McShane et al. [7] utilized Concanavalin A and dextran which were labeled with acceptor and donor dyes respectively. In the presence of glucose, the labeled dextran was displaced from the Concanavalin A resulting in a change in fluorescence. The sensors are being placed in microspheres, which have yet to be investigated for biocompatibility and to ensure that the toxic Concanavalin A does not leach out of the microspheres.

Carbon nanotubes have also been investigated as glucose sensors. Strano et al. [8] coated carbon nanotubes with a one-molecule-thick layer of sensing elements that react with glucose and changes the nanotubes' fluorescence. The coated nanotubes are encased within a thin capillary tube and implanted in the body. The capillary tube allows glucose to enter while preventing the nanotubes from contacting surrounding cells. However, long-term biocompatibility studies have not been performed.

1.2.2 Detection Equipments

A spectrofluorometer is an automatic scanning instrument that is used to study a substance's fluorescence over a wide range of wavelengths. The schematic diagram of a general spectrofluorometer is shown in Figure 1.6.

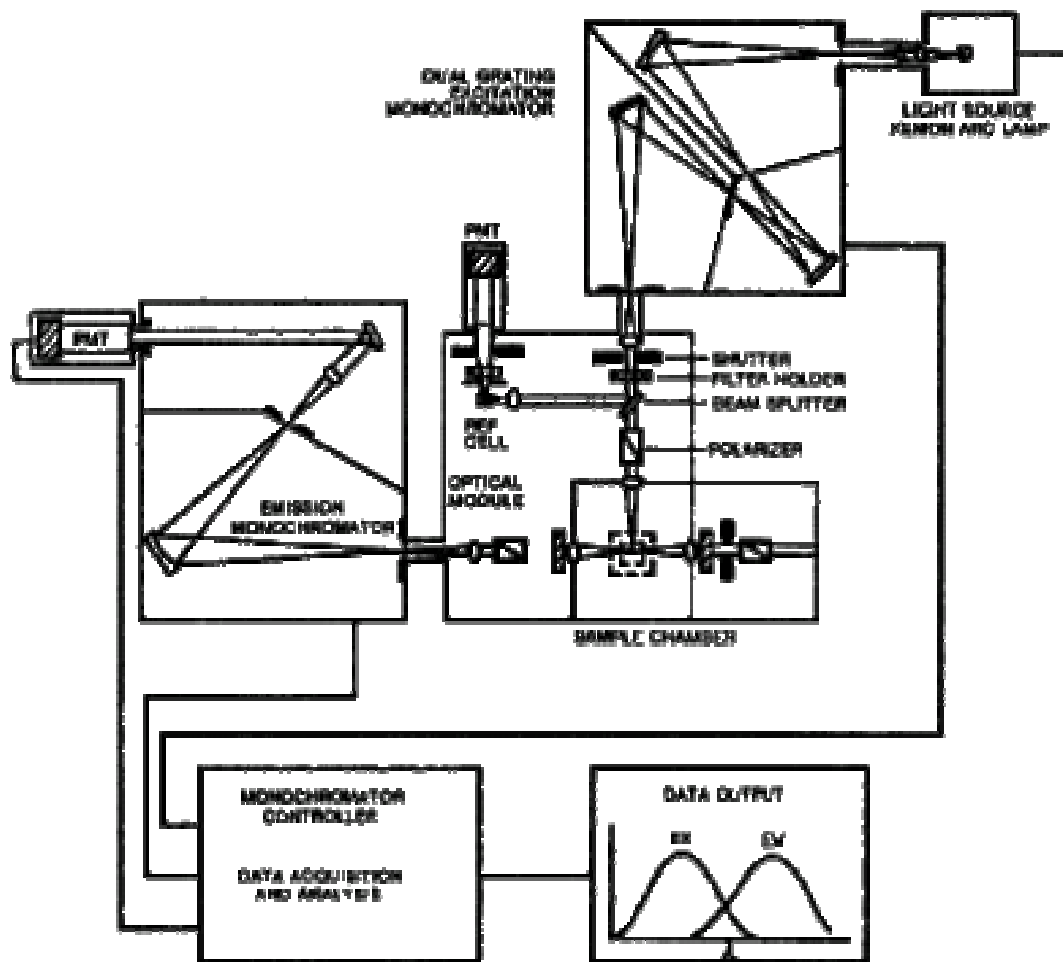


Figure 1.6 Schematic diagram of a spectrofluorometer [2].

The excitation light is usually a xenon arc lamp that has continuous high intensity at all wavelengths ranging upward from 250 nm. Monochromators with concave gratings are equipped to select both the excitation and emission wavelengths and decrease stray light to avoid problems caused by scattered

stray light. A monochromator has both an entrance and an exit slit. Larger slit widths cause higher signal-to-noise ratios. Also, to compensate for the monochromators, optical filters are used to maximize the sensitivity. Shutters are provided to delete the excitation light or to close off the emission channel, and a beam splitter reflects part of the excitation light to a reference cell. The fluorescence is detected with Photomultiplier tubes (PMTs) and the signal is quantified using electronic devices such as computers.

Photomultiplier tubes (PMTs) are widely used in spectrofluorometer. They can detect light from the UV to visible wavelength range. Advantages of PMTs include ultra-fast response, excellent energy resolution, low noise, and high gain. A schematic of a PMT is shown in Figure 1.7. They consist of a photocathode and a series of dynodes, which are the amplification stages in an evacuated glass enclosure [6]. Incident photons that strike the photoemissive cathode emit electrons due to the photoelectric effect, and the dynodes are also held at negative potentials that decrease toward zero along the dynode chain. The photocathode is held at a high negative potential (usually, -1000 to -2000 V). This potential difference leads to acceleration of an ejected photoelectron toward the first dynode. The photoelectrons are accelerated towards a series of additional electrodes, dynodes, until a current pulse arrives at the anode, generating additional electrons at each dynode. This cascading effect creates 10^5 to 10^7 electrons for each photon hitting the first cathode depending on the number of dynodes and the accelerating voltage. This amplified signal is finally collected at the anode where it can be measured.

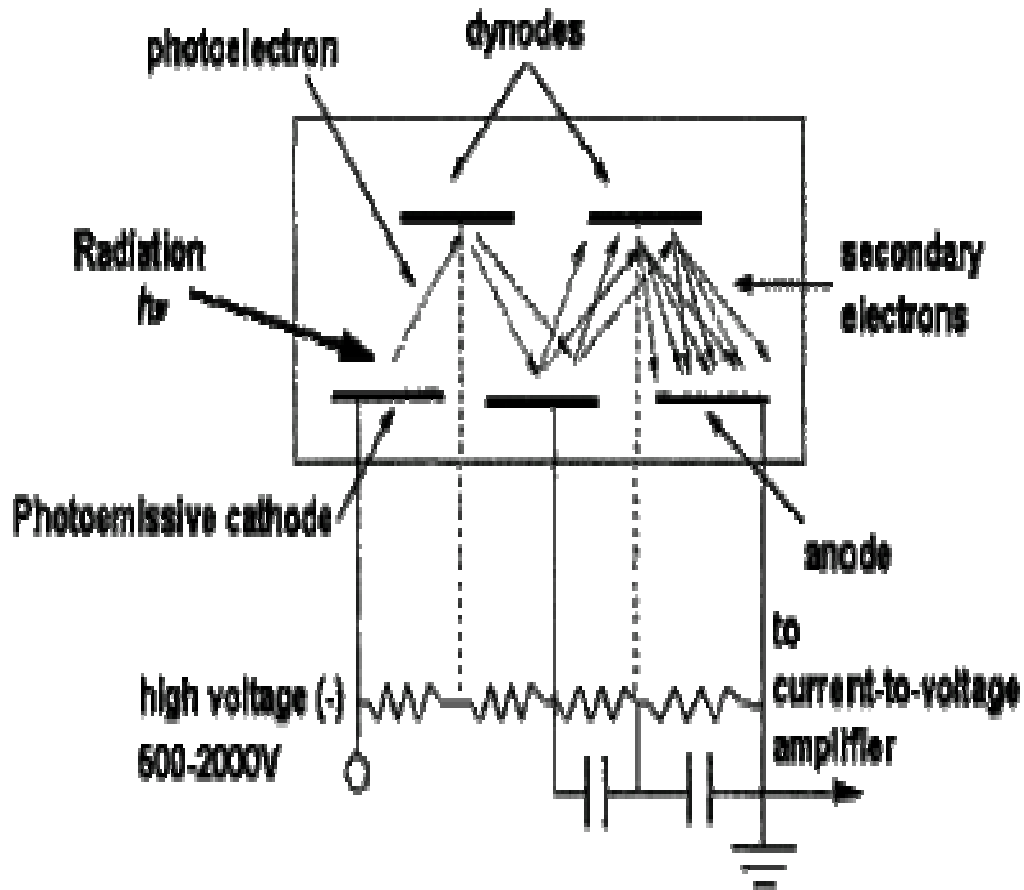


Figure 1.7 Schematic of a PMT [9]

Charge-coupled devices (CCDs) are imaging detectors with high sensitivity for measurement of low light levels and linear dynamic range [6]. They are also integrated-circuit chips containing an array of capacitors that store charge when light creates e-hole pairs. The charge accumulates in proportion to the total light exposure, and can be read out in a fixed time interval.

Photodiodes are P-N junctions that are specifically designed to optimize their inherent photosensitivity. A photodiode is a linear array of discrete

photodiodes on an integrated circuit (IC) chip that generates an output voltage that is proportional to the current flowing through a photodiode, which is in turn proportional to the light intensity falling on the photodiode. Light creates electron-hole pairs and the electrons migrate to the nearest PIN junction. Array detectors are especially useful for recording the full UV-VIS adsorption spectra of samples rapidly passing through a sample flow cell.

CHAPTER 2

INTRODUCTION

2.1 Background

Recently, increased focus has been placed upon the development of sensors and biosensor devices for the long-term monitoring and managing of health conditions. In particular, glucose sensors have been heavily investigated [10]. The main objective in these investigations has been to develop an ideal *in vivo* sensor with ultra-sensitivity, high selectivity, reliability, limited biofouling, and low cost. While those features could be found in some of the developed implantable sensors, biofouling imposed a major problem.

Implantable sensors suffer from biofouling [11]. Biofouling is caused by nonspecific adsorption of proteinaceous materials to the sensor surface [12]. This material will encapsulate the implantable device and render it inoperable. The encapsulation accrues a few days later when the fibroblasts cells migrate to the implant surface and contribute to the encapsulation process through proliferation, surrounding the implant to isolate it from the body. The result from the above effects is isolation of the sensing surface from the analyte which leads to delayed or inaccurate measurements. Medtronic, Inc (Minneapolis, MN) is producing an implantable electrochemical glucose sensor that could last for 72 hours.

There are several techniques for improving biocompatibility and thus reducing biofouling. For example, the use of polymeric materials such as membrane coatings to modify the surface charge and wettability of the sensor substrate has been investigated [13-19]. Quinn et al. [20] used brush polymer materials to modify the surface of a glucose sensor. Specifically the polyethylene glycol (PEG) chains were incorporated into polyhydroxyethylmethacrylate (PHEMA) membranes which resulted in less fibrous encapsulation after subcutaneous implantation in rats. However, long-term biocompatibility was still a problem.

Researchers have investigated biocompatible intracellular sensors. For example, Kopelman and his group have developed PEBBLES, probes encapsulated by biologically localized embedding, which are utilized as intracellular sensors to detect ions such as oxygen, chloride, and magnesium [21-24]. In one of their studies, a magnesium sensitive dye along with a reference dye was entrapped within a polyacrylamide matrix and inserted into C6 glioma cells for the development of an intracellular magnesium sensor.

To overcome biocompatibility problems, Red Blood Cells (RBCs) will be investigated. While RBCs have been utilized as carriers for therapeutic agents [25,26], they have not been used as carriers for glucose sensors. RBCs have potential advantages for use as glucose sensor carriers:

1. RBCs can transport glucose in and out of the cell for most species, except pig [27], and this transport is insulin independent;

2. the Hypo-Osmotic dialysis technique can quickly load a significant number of RBCs with probes resulting in a 93% survival rate and a normal mean cell life and cell half-life [28];
3. the mean RBC survival is 120 days;
4. RBC have no organelles including neither nuclei nor ribosome, thus RBCs can not synthesize new proteins and thus are designed to provide a milieu where enzymes remain functional for 120 days.

In this study, RBCs will be utilized to isolate the biosensor and result in fast response to glucose concentration.

2.2 Significance

Diabetes has become a wide spread disease not only among adults but also among children. Recent statistic from the American Diabetes Association (ADA) reported that 20.8 million people - 6.3% of the population - have diabetes, making it the fifth leading cause of death by disease in the U.S and also contributing to higher rates of morbidity [29]. People with diabetes are at higher risk for heart disease, blindness, kidney failure, extremity amputations, and other chronic conditions. In 2002, the ADA reported that direct medical and indirect expenditures attributable to diabetes were estimated at \$132 billion.

In July 2005 ADA reported about a new type of diabetes called slow-onset diabetes or diabetes 1.5, which has similarities both to type 1 and type 2. It is recognized as type 1.5, because at first, it looks like and reacts positively to treatments for type 2. However, it ends up revealing itself as an autoimmune form of diabetes, more like type 1.

Diabetics must closely monitor their glucose levels in order to avoid the detrimental effects of the disease. A glucose meter is utilized by patients pricking their finger (up to 7 times a day) and placing a drop of blood on a test strip to determine glucose concentration. An implantable glucose sensor that could be interfaced with an implantable insulin pump would provide a closed loop for an automatic control of glucose levels.

Successful implementation of our technology will help advance the science of glucose monitoring and managing. The innovation of nanocellular glucose biosensor arises, not from the fluorescent probes, but from the insertion of the probes into the RBCs. If successful, our group will be the first to report on the utilization of RBCs as biocompatible transports for glucose sensors. Additionally, this technique can be applicable to other analytes of interest such as cortisol which can also diffuse through RBCs. A disclosure on our technique has recently been filed.

2.3 Objective

This study will use the merger of two techniques: FRET competitive binding or conformational change methods and hypo-osmotic dialysis of RBCs in order to develop a novel RBC/nanoprobe glucose sensor. The objectives of the study are:

1. Development of glucose nanobiosensors using competitive binding technique.
2. Improvement of glucose sensing by testing different dextran sizes.
3. Identifying and testing new FRET pairs.
4. Investigation of Near Infra Red (NIR) FRET pair.
5. Development of new glucose nanobiosensor utilizing protein's conformational change.
6. Encapsulation of nanoprobes in RBCs.
7. Encapsulation of glucose nanobiosensors in RBCs.
8. Signal detection from encapsulated RBCs through tissue.

These techniques offer the advantages of:

1. Reducing sensor incompatibility by utilizing RBCs as protective, biocompatible carrier,
2. Providing a stable, specific response to glucose through the utilization of FRET nanoprobes and avoiding the need for nanospheres which can suffer fabrication uniformity and leaching.

3. Long-term sensor which is more convenient and less invasive than current sensors used.

The utilization of RBCs could become a revolutionary technique to monitor glucose and other analytes.

CHAPTER 3

NANOPROBE DEVELOPMENT

3.1 Optical Glucose Nanoprobes Development

3.1.1 Introduction

Glucose sensing development is a very active research area. One ultimate goal of researchers is to develop and fabricate an implantable glucose sensor. The development of a glucose sensor starts with developing a probe that responds well to glucose. This project will provide ideas and experiments to fulfill the development of such a sensor.

The main objective of this investigation was to determine if AF750 and AF680 is a viable FRET pair for implantable glucose biosensor. Three experiments were performed:

- 1) AF750 and AF680 were labeled to streptavidin and biotin and the energy transfer was determined;
- 2) AF750 and AF680 were labeled to Con A and dextran (MW 3000 and MW 10,000) and glucose response was determined in a spectrofluorometer;
- 3) AF750 and AF680 were labeled to Con A and dextran (MW 3000) and glucose response was determined through porcine skin.

These experiments help facilitate improvement in the development of an implantable biosensor to monitor glucose.

A biosensor is the utilization of a protein or enzyme for detection. There are several enzymes and proteins with high affinity to glucose such as Glucose

Oxidase (GOx), Glucose Dehydrogenase (GDH), Concanavalin A (Con A), and others. These enzymes have been used by other researchers to detect glucose. In this project, those enzymes will be tested as a part of nanoprobe development which will be encapsulated in RBCs.

This biosensor development will detect changes optically. This requires study of the different fluorescence properties. Since this nanobiosensor will operate *in vivo* and FRET technique will be implemented, there will be a selective list of fluorophores to be viable for use. The FRET study will be conducted by using the high binding affinity between Streptavidin and Biotin.

3.1.2 FRET Method of Detection

FRET is a distance dependent technique. This distance is called Förster radius (R_0). It is the distance at which energy transfer is 50% efficient (i.e., 50% of excited donors are deactivated by FRET). The magnitude of R_0 is dependent on the spectral properties of the donor and acceptor dyes [30-36]. To ensure that close proximity of the two dyes, we have to select molecules with high affinity to each other. Streptavidin and Biotin have high binding affinity [37]. This binding affinity will allow the labeled sites with the two dyes to be in close proximity.

3.1.3 Streptavidin and Biotin as Biologic Markers

Biologic markers are good testing indicators. Streptavidin and Biotin are considered as biologic markers due to their high binding affinity. They were first exploited in histochemical applications in the mid-1970s [38, 39]. They are used

for diverse detection schemes [40-41]. In their simplest form, such methods entail applying a biotinylated probe to a sample and then detecting the bound probe with a labeled streptavidin. In some applications, immobilized streptavidin is used to capture and release biotinylated targets.

Streptavidin

Streptavidin is a nonglycosylated protein with a near-neutral isoelectric point. Its molecular weight is 52,800-dalton. Streptavidin contains the tripeptide sequence Arg–Tyr–Asp (RYD) that apparently mimics the Arg–Gly–Asp (RGD) binding sequence of fibronectin, a component of the extracellular matrix that specifically promotes cellular adhesion [42]. This universal recognition sequence binds integrins and related cell-surface molecules (Figure 3.1).

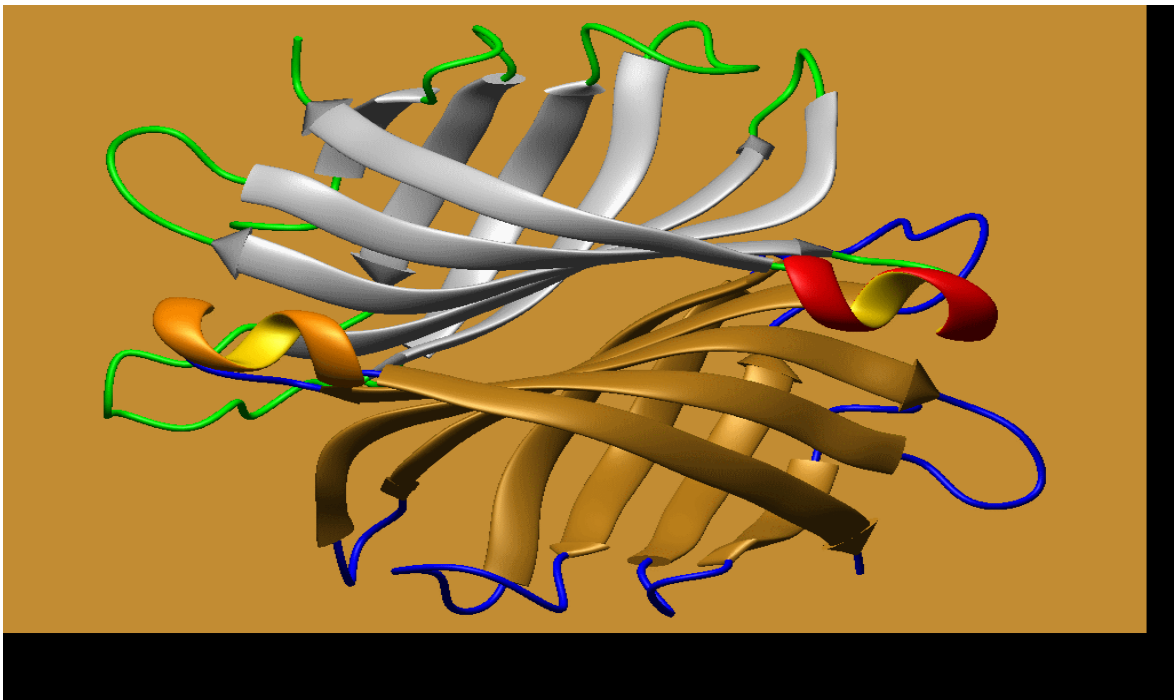


Figure 3.1 Structure of Streptavidin [43]

Biotin

Biotin is a 14-atom spacer. Biotin has a molecular weight of 12,000 Dalton. It has been shown to enhance the ability of the biotin moiety to bind to avidin's relatively deep binding sites.

Binding Characteristics of Biotin-Binding Proteins

Streptavidin biotin-binding protein binds four biotins per molecule with high affinity and selectivity. Dissociation of biotin from streptavidin is reported to be fast [44]. The multiple binding sites permit a number of techniques in which unlabeled streptavidin biotin-binding protein can be used to bridge two biotinylated reagents. This bridging method is commonly used to link a biotinylated probe to a biotinylated enzyme in enzyme-linked immunohistochemical applications (Figure 3.2).

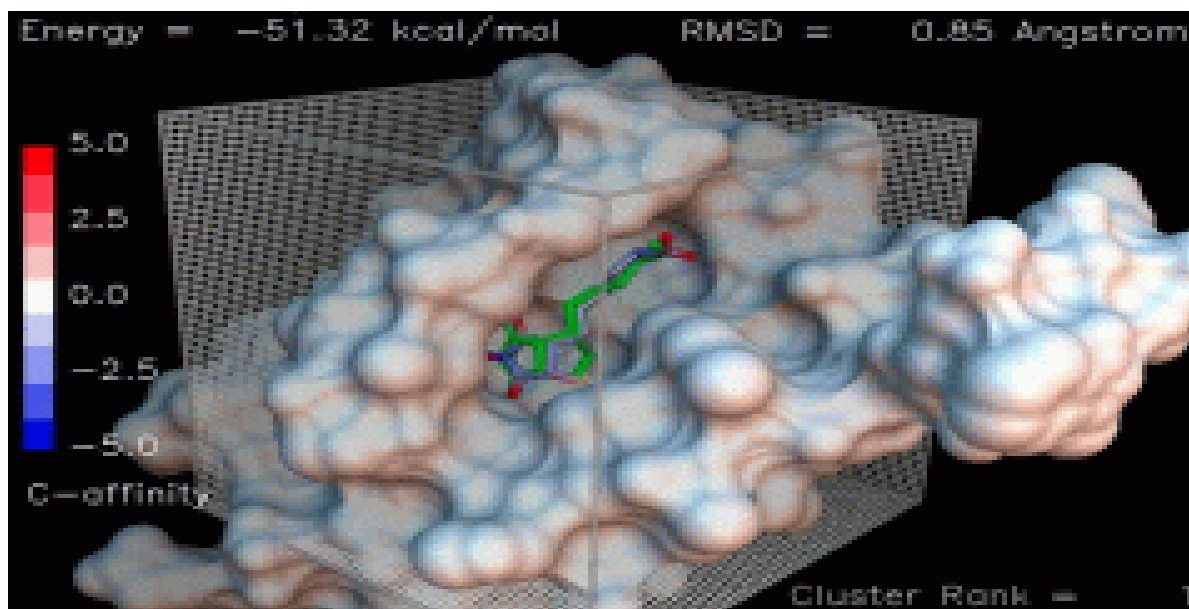


Figure 3.2 Streptavidin biotin-binding protein binding [45]

3.1.4 Chosen FRET Fluorophores

Alexa Fluor 750

Alexa Fluor 750 dye is the longest wavelength Alexa Fluor dye currently available (Figure 3.3). Its spectrum is similar to Cy7 dye. Its fluorescence emission maximum at 779 nm is well separated from commonly used far-red fluorophores such as Alexa Fluor 647, Alexa Fluor 660, or allophycocyanin (APC), facilitating multicolor analysis. With a peak excitation at ~752 nm, conjugates of the Alexa Fluor 700 dye are well excited by a xenonarc lamp or dye-pumped lasers operating in the 720–750 nm range [46].

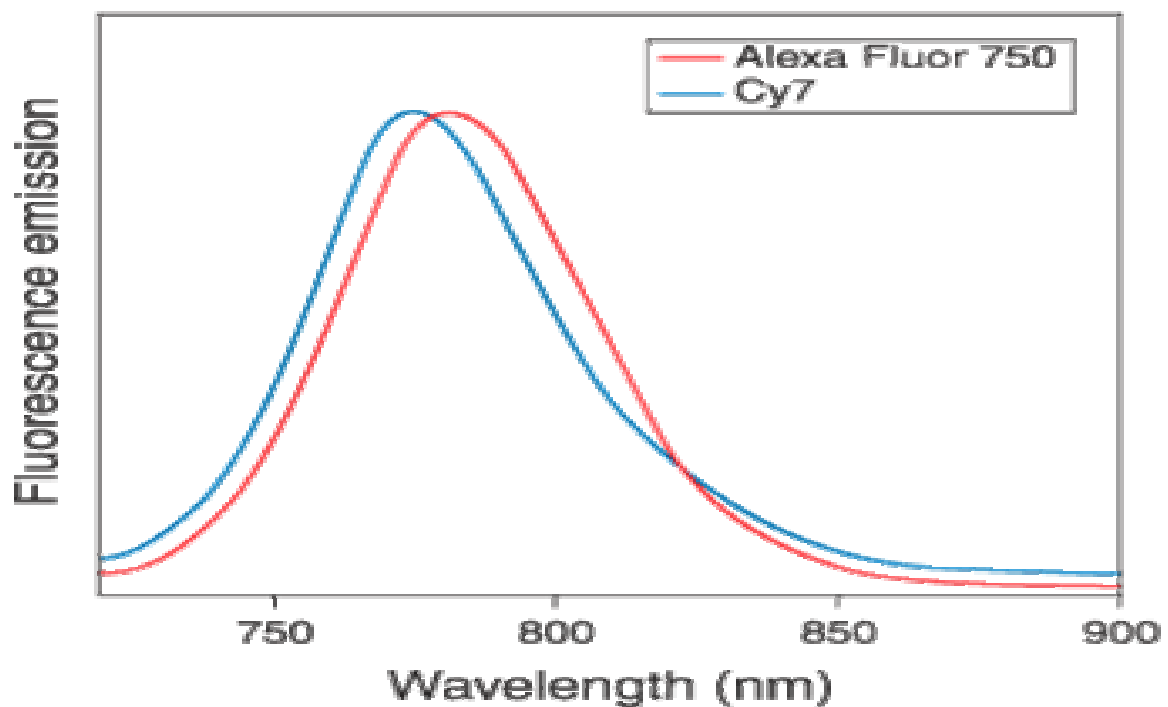


Figure 3.3 Emission spectrum of AF 750 and Cy7 [46]

Alexa Fluor 680

With a peak excitation at 679 nm and maximum emission at 702 nm, the Alexa Fluor 680 dye is spectrally similar to the Cy5.5 dye (Figure 3.4). Fluorescence emission of the Alexa Fluor 680 dye is well separated from that of other commonly used red fluorophores, such as the tetramethylrhodamine, Texas Red, R-phycoerythrin, Alexa Fluor 594, and Alexa Fluor 647 dyes [47].

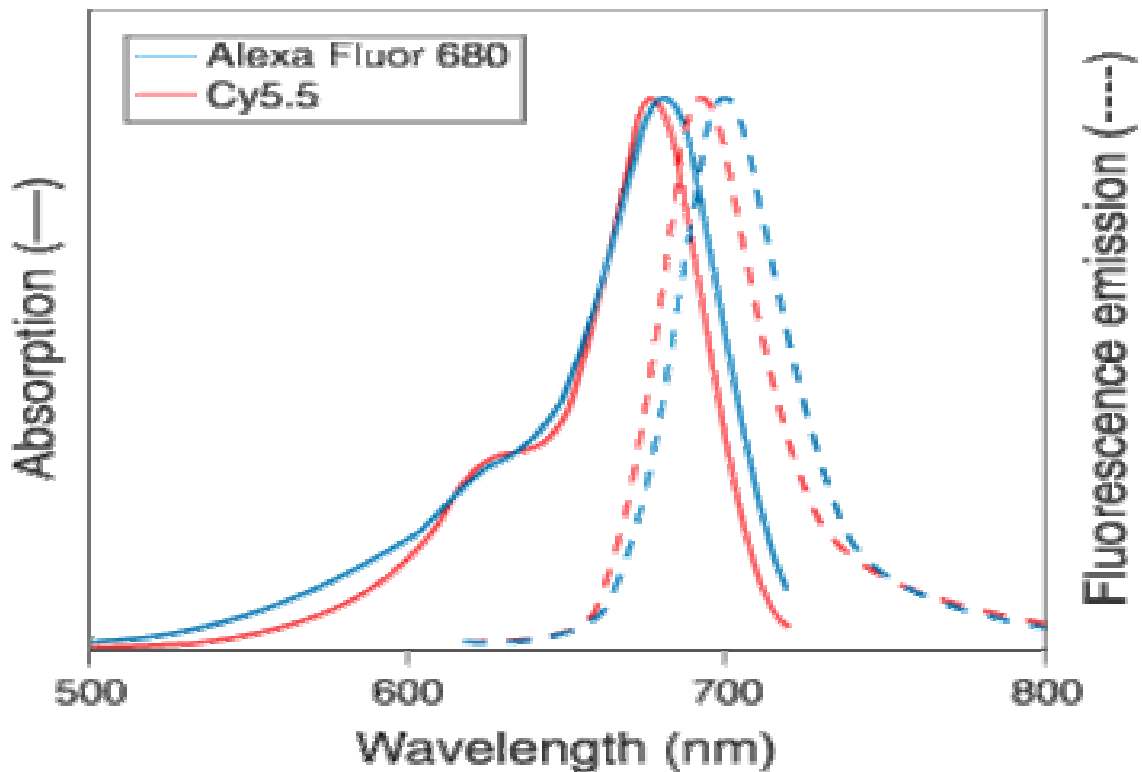


Figure 3.4 Emission and Absorption spectrum of AF 680 and Cy5.5 [47]

3.1.5 Chosen Competitive Binding Markers

Dextran

Dextran is a polymer of anhydroglucose. It is composed of approximately 95% α -D-(166) linkages. Native dextran has a molecular weight (MW) in the range of 9 million to 500 million [48-50]. Dextrans with lower MW have fewer branches [51] and have a more narrow range of MW distribution [52]. Dextrans with 10,000 MW or greater behave as if they are highly branched. As the MW increases, dextran molecules attain greater symmetry [53,54]. Dextrans with MW of 2,000 to 10,000, exhibit the properties of an expandable coil. At MW below 2,000, dextran is more rod-like [55] (Figure 3.5).

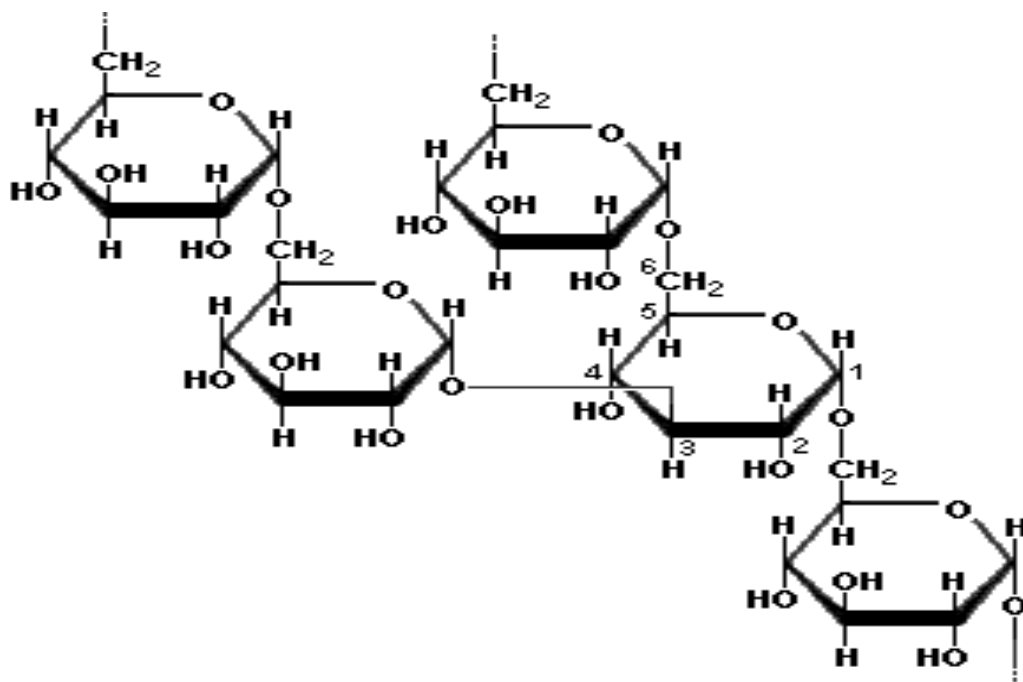


Figure 3.5 Structure of dextran molecule fragment [56]

Fluorescence labeled dextran is used extensively in microcirculation and cell permeability research utilizing microfluorimetry [57, 58]. FITC-dextran has been used to study plant cell wall porosity and capillary permeability [59]. In this study, optimization of the base line and maximum FRET is the objective. We will study the affect of two different MW dextrans on glucose response.

Concanavalin A

The molecular structure of Concanavalin A (ConA) is composed of identical subunits of 237 amino acid residues (M.W.: 26,000) with no covalently bound carbohydrate or other prosthetic group [60].

ConA reacts with non-reducing α -D-glucose and α -D-mannose - it is the ring form that participates in the reaction. The α -methyl-D-glucopyranoside acts as a competitive inhibitor [61].

Diabetes is a world-wide disease. According to the ADA by the year 2020, there will be 250 million people afflicted with this disease. Most diabetics monitor their glucose levels at least several times a day, followed by appropriate actions to maintain normal glycemia. Stricter monitoring of glucose level would help prevent some of the adverse health effects associated with diabetes. Ideally, an implantable glucose sensor would reduce the pain associated with the finger stick testing while also maintaining strict control over blood glucose levels. Currently, the commercially available test kits utilize electrochemical sensors that require extraction of a sample of blood.

Recently, increased focus has been placed upon the development of sensor and biosensor devices for long-term monitoring and managing of diabetes [62, 63]. Many scientists are investigating glucose sensors based on fluorescence spectroscopy. It has the advantages of high sensitivity and superior specificity provided by molecular recognition [64]. In fact, there are many fluorescent probes that monitor glucose accurately. For example, a series of experiments were performed using FRET and competitive binding technique. McShane et al. [66] utilized Concanavalin A and dextran which were labeled as acceptor and donor dyes respectively. In the presence of glucose, the labeled dextran was displaced from the Concanavalin A resulting in a change in fluorescence. Glucose concentration can be estimated from FRET efficiency, and the ratiometric nature of the FRET analysis method allows compensation for variations in instrumental parameters, assay component concentrations, and measurement configuration [65]. By using AF750 and AF680 as an IR FRET pair, we will be able to design *in vivo* sensors.

For fluorophores to be utilized as implantable sensors, high quantum yield and near IR emission (NIR) would be ideal, but such a combination is not currently available because red and NIR dyes generally have a lower quantum yield than shorter-wavelength dyes. On the other hand, NIR dyes make use of the tissue window. The judicious choice of the FRET dyes is critical in the development of an optical implantable glucose sensor. In this study, it was hypothesized that the fluorophores Alexa Fluor 750 and Alexa Fluor 680 would be a viable choice for an implantable FRET biosensor for glucose detection.

Typically, the FRET fluorophore molecule pairs are characterized via the Förster radius (R_0), which is the distance at which energy transfer is 50% efficient (i.e., 50% of excited donors are deactivated). In this study, to ensure that close proximity of the two dyes (0.5 to $2 R_0$), molecules with high affinity to each other were utilized. Thus, streptavidin and biotin were labeled to the fluorophores. Streptavidin biotin-binding protein binds four biotins per molecule with high affinity and selectivity. Dissociation of biotin from streptavidin is reported to be fast, $2.4 \times 10^{-6} \text{ s}^{-1}$ [66].

Additionally, glucose sensing was conducted using this FRET pair. Dextran is an inhibitor to Con A. When glucose is added to the solution of dextran and Con A bound, glucose will displace dextran and binds to the Con A. This displacement will take place due to the high affinity of glucose to Con A. As result of the displacement there will be change in FRET.

3.2 Materials and Methods

Materials

Concanavalin A (5 mg/ml), sodium bicarbonate (84.01 MW, 0.1 M, pH 8.3), bovine serum albumin (2 mg/ml, pH 7.0), phosphate buffered saline (0.01M, pH 7.4), and beta-D(+) glucose (180.2 MW, 100 mg/ml) were purchased from Sigma (St. Louis, MO). Streptavidin-Alexa Fluor 680 (52,800 MW, 1mg), Alexa Fluor 680-dextran (molecular weight 10,000 Da, 1 mol AF680/mol of dextran & molecular weight 3000 Da, 1 mol AF680/mol of dextran), Alexa Fluor 750 carboxylic acid (succinimidyl ester, 1 mg), and FluoReporter Mini-biotin-XX

protein labeling kit (5 labeling of 0.1-3 mg protein each) were purchased from Invitrogen (Carlsbad, CA). Dialysis tubing (6000-8000 MWCO) was purchased from Fisher Scientific (Hampton, NH). DMSO 78.13 MW was obtained from MU Recycling (MU Recycling – D-5879 – lot 100F-0269). Dialysis tubing 6000-8000 MWCO was purchased from Fisher Scientific (Fisher Scientific – 21-152-3). PBS 0.01M, pH 7.4 (Sigma - P-3813 - lot 075K8206), Beta-D(+) glucose 180.2 MW, 100 mg/ml (Sigma, G5250, Batch # 014K1265), and BSA 2 mg/ml, pH 7.0 (Sigma – G2133 – lot 034K1462) were all purchased from Sigma. AF680-dextran (molecular weight 10,000 Da, 1 mol AF680/mol of dextran & molecular weight 3000 Da, 1 mol AF680/mol of dextran) was purchased from Invetrogyn.

Instrumentation

A UV-Vis absorbance spectrometer (Beckman DU 520) was used to collect absorbance spectra and perform catalytic activity tests. The slit size (4 nm) and scanning speed (595 nm/min) were held constant throughout all the experiments. A scanning fluorescence spectrometer (FluoroMax-3 Jobin Yvon, Hobira) was used to collect fluorescence emission spectra by exciting the sample at 749 nm. The slit size and integration time were 5 nm and 0.5 s, respectively.

Preparation of Biotin

BSA 0.5 mg/ml was used in the biotinylation. It was dilute 10 mM sodium phosphate buffer. Using the labeling kit protocol form Molecular Probes will use the resulted stock in the labeling with AF750.

Bio-Rad experiment was conducted to determine the final protein concentration and the degree of labeling. The final BSA-Biotin concentration was 1.103 mg/ml and the degree of labeling (DOL) was determined by the use of UV-VIS. The labeled BSA was scanned and the absorbance at 749 nm was determined. The DOL was calculated according to this formula

$$\text{DOL} = (A_{\text{max}} \times \text{MW}) / ([\text{Protein}] \times \epsilon_{\text{dye}})$$

The DOL was 0.8. This means that for every mole of protein there is a mole of dye and the AF680-streptavidin DOL is 3.

Preparation of Con A

The Con A from Sigma was in powder form. Con A (10 mg) was labeled with AF750 following the protocol provided by Molecular Probes.

Bio-Rod experiment was conducted to determine the final protein concentration and the degree of labeling. The final Con A concentration was 9.86 mg/ml and the degree of labeling (DOL) was determined by using UV-VIS. The labeled Con A was scanned and the absorbance at 749 nm was determined. The DOL was calculated according to this formula

The DOL was 2.94 mole of dye/ mole of Con A. This means that for every mole of protein there is approximately 2.94 moles of dye. The AF680-dextran DOL is 1 mole of AF680 for every mole of dextran.

FRET Experiments using AF680 and AF750

Biotin and Streptavidin have strong binding affinity for each other. Since biotin is a small molecule, BSA was biotinylated and then labeled with AF750. The binding affinity between the biotinylated BSA-AF750 and AF680-streptavidin was used to allow AF750 and AF680 to be in close proximity. This distance has to be between 20 and 100 Å. When that condition is fulfilled and also an overlap between the donor, AF680, emission spectrum and the acceptor, AF750, excitation spectrum take place then this will result in FRET. The observation of FRET was conducted by the addition of 1ug AF750-BSA to the solution of the 1ug AF680-streptavidin in PBS. The total volume was 3ml. The 1ug AF680-streptavidin, donor, in PBS was scanned to determine its peak without AF750-BSA, acceptor. When the acceptor was added, there was a drop in the donor peak as the sample was excited at 680 nm.

The experiments were conducted in 4 ml cuvettes. The spectrofluorometer was adjusted to 1 nm increments and an integration time of 0.5 seconds. The excitation was set at 680 nm. 1 ug of BSA-AF 750 was scanned by setting the excitation at 750 nm and the slits at 5. FRET was determined by placing 1 ug of AF680-streptavidin in a cuvette. PBS was added and a scan was conducted to acquire the sample background without AF750-BSA biotin. Next, 1 ug AF750-BSA biotin was added to the cuvette and more spectra were obtained. Energy transfer from the AF680-streptavidin (donor) was determined. The final sample was 1 ug AF750-BSA biotin in 1 ug AF680-streptavidin in 1 ml PBS.

FRET Experiments via dextran size testing for glucose response

Since AF680 and AF750 proved to be a useful FRET pair dye, it was used in all future experiments for detecting glucose. Con A is considered as a glucose binding protein. Dextran binds to Con A but with lower affinity than glucose. By using the binding property of dextran to Con A and then introducing glucose to the sample, due to the higher affinity of glucose to Con A, dextran will be displaced. This property is called competitive binding. This displacement will provide a change in FRET.

In previous experiments of probes development, researchers utilized large chains of dextran, whose molecular weight ranged from 500,000 to 2,000,000 MW. In this experiment, we tested the effect of dextran size on the glucose detection by using the competitive binding technique. There were two sizes of dextran selected, 10,000 MW and 3000 MW.

All experiments in this section were conducted in 4 ml cuvettes. The excitation was set at 680 nm, which is the excitation wavelength for the AF680-dextran. The increment was set at 1nm and the integration time was at 0.3 s. The slits were opened to 7.

The test on the dextran with (10,000 MW) was conducted by placing 0.1 ug of AF680-dextran in a 4 ml cuvette. Then PBS was added. The total volume was 3 ml. A scan of the sample was conducted to acquire the background without AF750-Con A. Then 0.2825 ug of AF750-Con A was added to the same cuvette. A scan of the sample was performed to determine the percent of energy transfer from the FRET pair. The mole ratio was maintained at 4 moles of dextran

to 1 mole of Con A. The same test was conducted with the same mole ratio 4:1 by using the dextran (3000MW). 0.1 ug of AF680-dextran and 0.789 ug of AF750-Con A were placed in a 4ml cuvette. Similar scans were obtained.

After 2 hr incubation to allow binding of the dextran to Con A, each sample was tested for glucose response. The test consisted of four additions of glucose concentrations from 0.016 to 0.397 uM. These glucose concentrations did not fall in the normal blood glucose concentration range in human, which range between 4.3 to 9 mM. Ten minutes was allowed for incubation with the glucose after each addition before scanning. This incubation time allowed full displacement of glucose to dextran. These experiments were conducted four times in order to obtain statistical data.

Transmission Studies of FRET glucose sensors through porcine skin

The main objective from using NIR dye is to be able to detect signal from an implantable biosensor. Skin is a barrier between the sensor and the detector. By placing a porcine tissue in front of the cuvette holder, this will mimic signal transmission from the sensor through skin. Porcine skin (4.06 mm thickness) was utilized. The biosensor probes from previous experiment of glucose response was used and then scanned. This experiment was followed by more testing with different tissue thicknesses to determine the relation between the tissue thickness and the fluorescence signal.

3.3 Results and Discussion

3.3.1 Fluorescence Resonance Energy Transfer (FRET) Experiments

In the following graphs, the results of the FRET streptavidin/biotin experiments are shown. Figure 3.7 shows the scan of the maximum peak of 1ug SA-AF680, donor without the presence of the BSA-AF750, acceptor. The excitation was set at 750 nm and the slits opening were at 5. The scan of the 1 ug of SA-AF680 gave a maximum peak of 1499411 cps at 702 nm. This peak represents the maximum emission of the AF680 when the donor is not present in the sample.

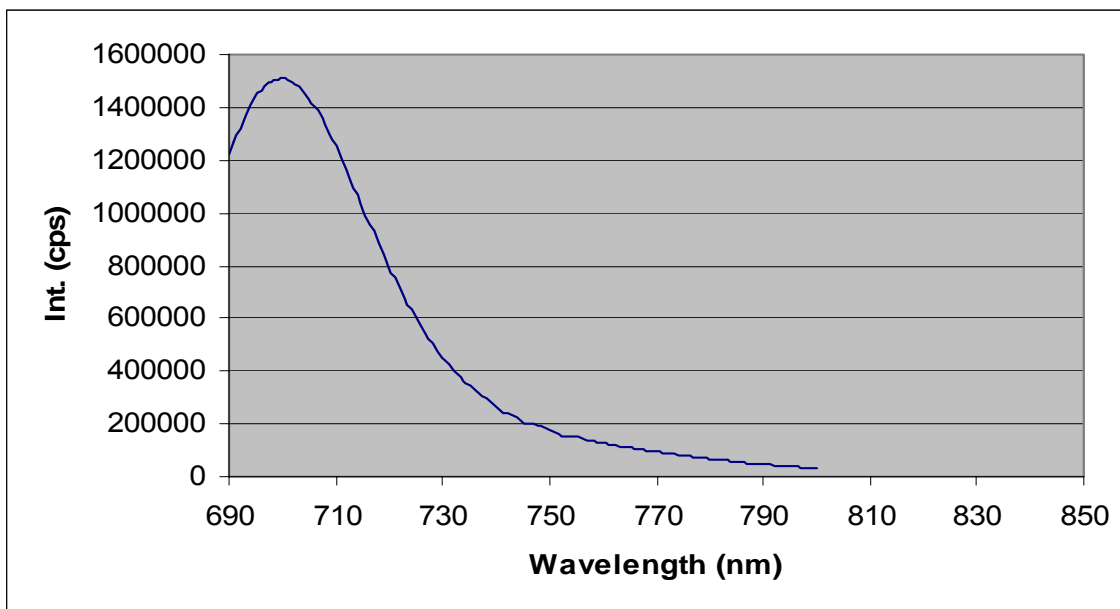


Figure 3.7 Scan of SA-AF 680 without the presence of BSA Biotin-AF 750

Next, the sample was scanned with the presence of the acceptor. The excitation was set at 680 nm and the slits opening were at 5. Figure 3.8 provided

peak of the donor with the presence of the acceptor which was 63624 cps at 702 nm.

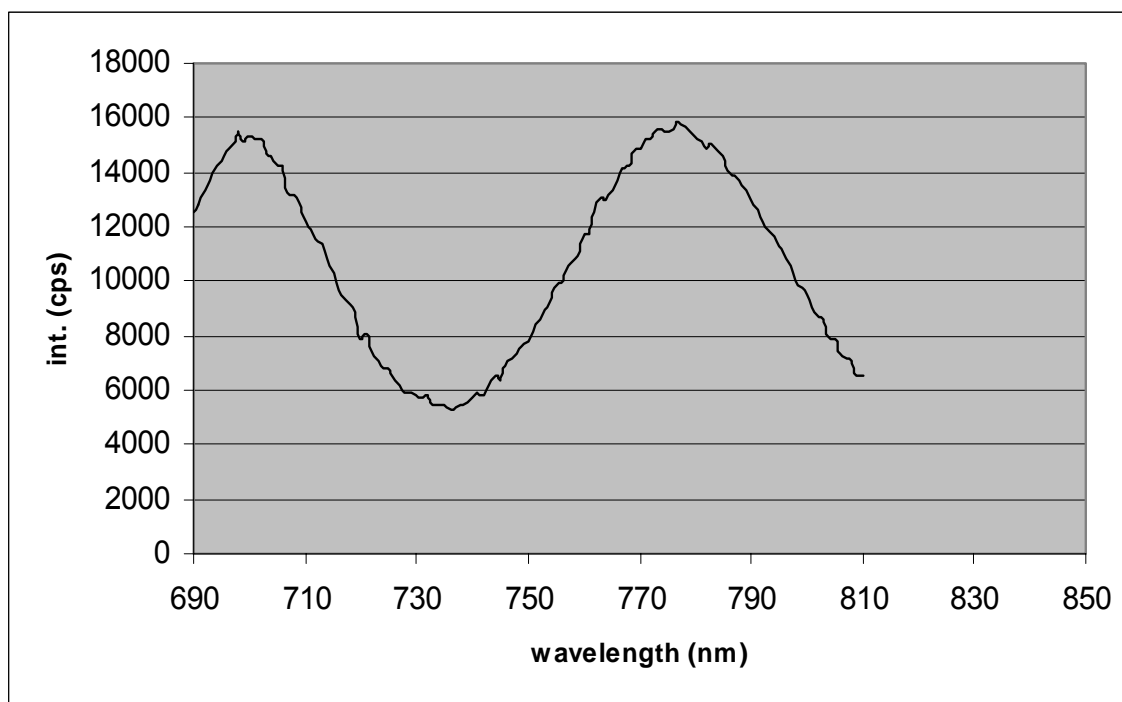


Figure 3.8 Scan of SA-AF 680 with the presence of BSA Biotin-AF 750

The energy transfer was calculated using equation (3 -1):

$$\% \text{ Energy transfer} = 1 - I_{DWA} / I_D \quad (\text{eqn 3.1})$$

where I_D is the donor's intensity without the presence of the acceptor and I_{DWA} is the donor's intensity with the acceptor presence. The results provided conclusive observations of energy transfer in term of increase in the acceptor peak and decrease in the donor peak. The energy transfer result was 95.76 %.

This result provided conclusive observations of energy transfer between the AF680 and AF-750 which will be used in future experiments as an NIR FRET pair.

3.3.2 Results of Dextran Size Effect on Glucose Response

Since the previous experiments determined that AF680 and AF750 fluorophores are viable FRET pairs, the next step was to utilize the fluorophores in a FRET-based glucose biosensor. First, two different molecular weight dextrans were examined. The two different sizes, MW 10,000 and MW 3000, of the labeled dextran had similar concentration and F/P ratio. In these experiments, four moles of dextran to one mole of Con A was maintained. This ratio increased the probability of dextran to bind to one or more of the four-sugar binding sites on Con A.

Figure 3.9 shows the glucose response when the dextran (10,000MW) was used. A high concentrated glucose was prepared to use for the additions. Those additions were added in smaller volumes to prevent any dilution effect. Then the donor/acceptor fluorescence ratio was calculated.

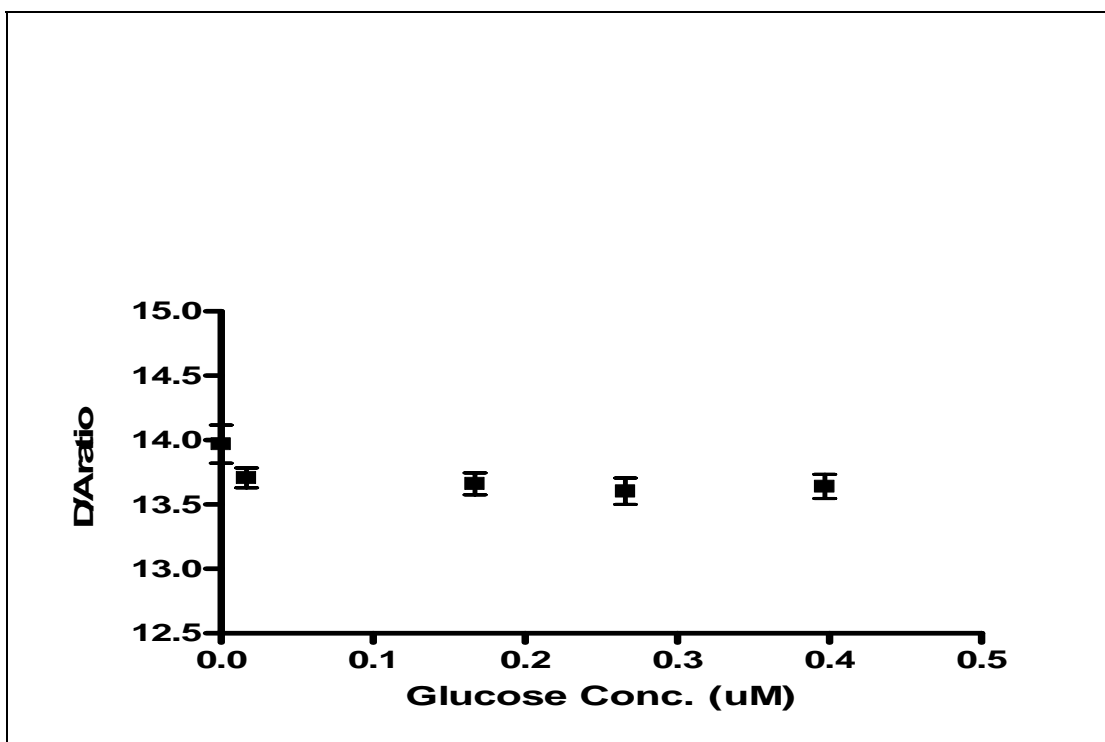


Figure 3.9 Glucose Response of AF680-dextran (10,000MW) and AF750-Con A.

The data was plotted as D/A ratio vs. glucose concentration, there was an inconsistency in the decrease of the D/A ratio as the glucose concentration was increasing. The response basically had a flat slope after the initial addition of glucose due to the low sensitivity.

The above data is representation of the inconsistency distance change between the donor and the acceptor. After the first addition, it seems that the distance between the donor and acceptor decreased since there was a drop in the donor signal and increase to the acceptor signal. However after the second addition the donor increased and the acceptor decreased. This means that the distance between the donor and the acceptor decreased.

In Figure 3.10, the glucose response is shown for the 3000 MW dextran. Unlike the results from using the higher molecular weight dextran (10000MW), there was an exponential decrease of the D/A ratio as the glucose concentration was increasing. Also the change in D/A ratio was small due to the small change in the glucose concentration.

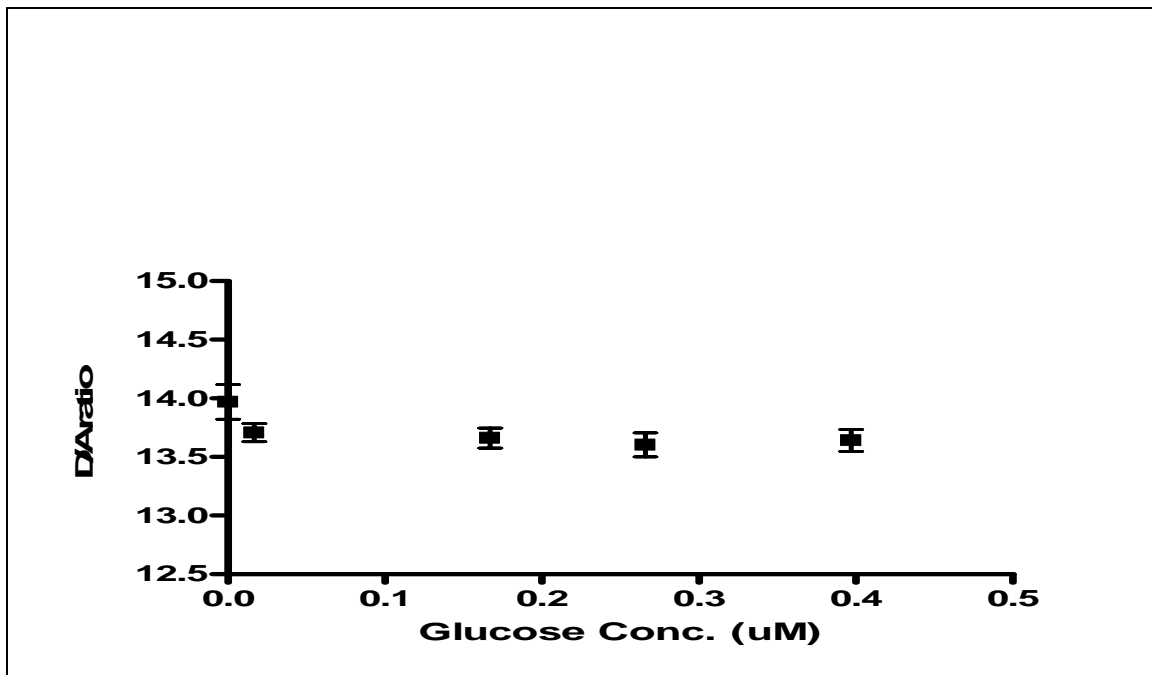


Figure 3.10 Glucose Response of AF680-dextran (3000MW) and AF750-Con A

Figure 3.9 shows an average of all four experiments performed. For the first glucose addition of 0.016 μM , there was a drop in the D/A peak ratio then there was an increase followed by a decrease in the D/A ratio. This inconsistency in responding to different glucose concentrations would make it difficult to monitor glucose concentration change. On the other hand, Figure 3.10 shows an average

of four experiments results with exponential decrease of the D/A ratio peak as the glucose concentration increase. It is possible that this inconsistency in glucose response when larger dextran was used is due to large sugar branch. Since there is no control over the sites to label on the dextran molecules, the smaller the dextran molecules the higher the possibility would be to label a site that could be in close proximity to the labeled binding site on the Con A.

Figure 3.11 was used to determine the mathematical representation of the behavior of the response. The exponential equation is

$$y = 14.076 e^{-0.0069 x}$$

The R^2 is 0.6831.

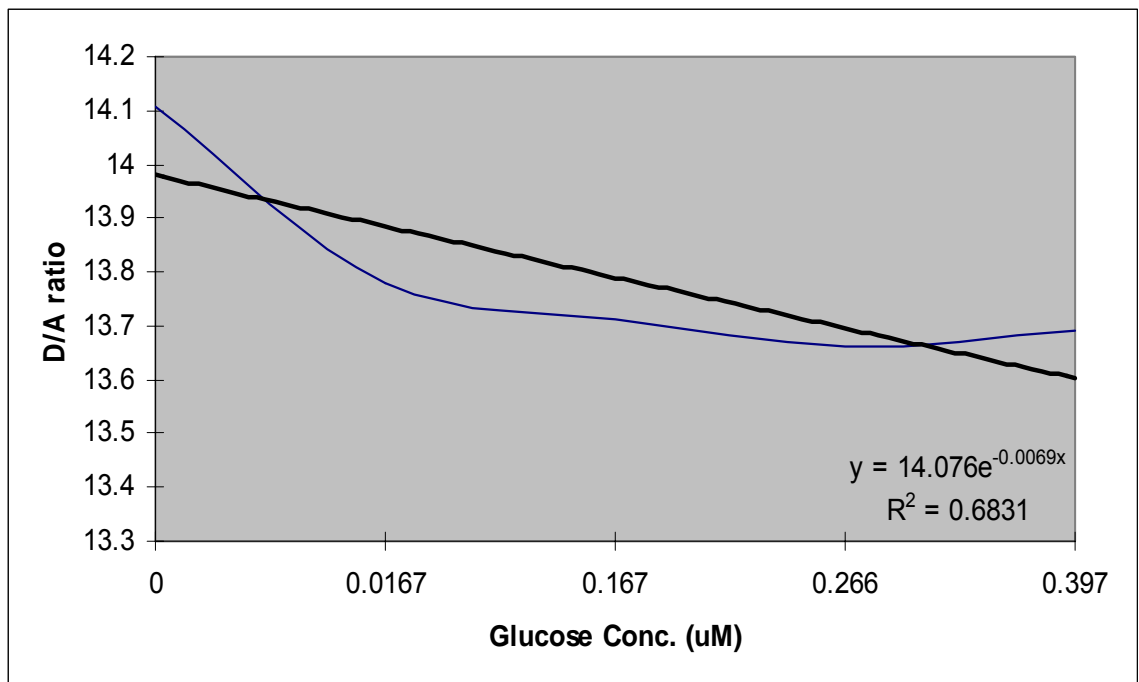


Figure 3.11 Graph for determining the exponential function.

The detection range was calculated in accordance to the number of moles of dextran and Con A in the sample. Therefore by using 0.1 ug of AF680-dextran (3000MW) and 0.789 ug of AF750-Con A in a 4 ml cuvette with 3 ml PBS added, 0.397uM of glucose concentration would be the maximum detection range. To improve this detection range, an adjustment can be made by adjusting the amount of AF680-dextran and AF750-Con A.

Figure 3.12 shows the average results of AF680-dextran (3000MW) and AF750-Con A after increasing the concentration of dextran and Con A. In these experiments, 0.2 ug of AF860-dextran with 2988 ul PBS was placed in a 4ml cuvette, and then 105.7 ug of Con A was added. These samples were incubated for 2 hours. The glucose concentration range in this test was between 3.33mM and 33.65mM.

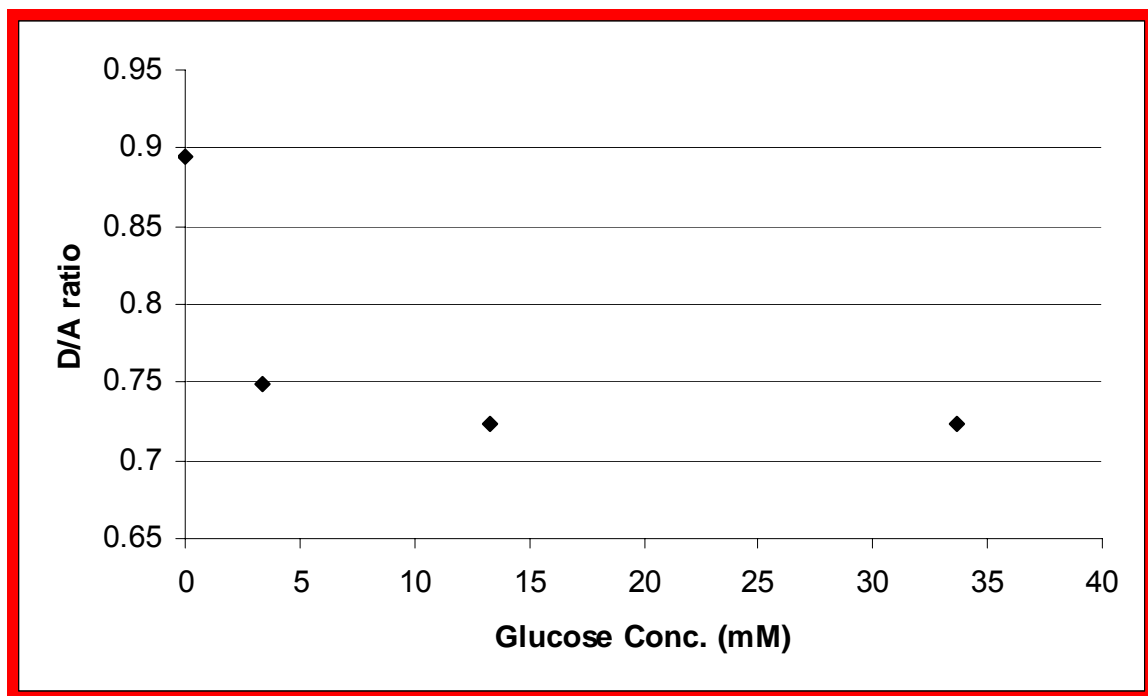


Figure 3.12 Glucose Response of AF680-dextran (3000MW) and AF750-Con A with larger detection limits

The maximum tested range exceeds the normal human blood glucose concentration. Again Figure 3.12 shows the exponential decrease to the peak of the D/A ratio as the glucose concentration increase.

3.3.3 Results of the Transmission Studies of FRET Glucose Sensors Through Porcine Skin

Implantable glucose sensors require the capture of transmitted glucose signal response through skin. In this experiment porcine skin was used to determine how much signal can be transmitted through it. A 4.06 mm thick porcine skin was place in front of the cuvette holder. Figure 3.13 shows results of the experiments with dextran (10,000MW) and (3000MW) with and without the tissue.

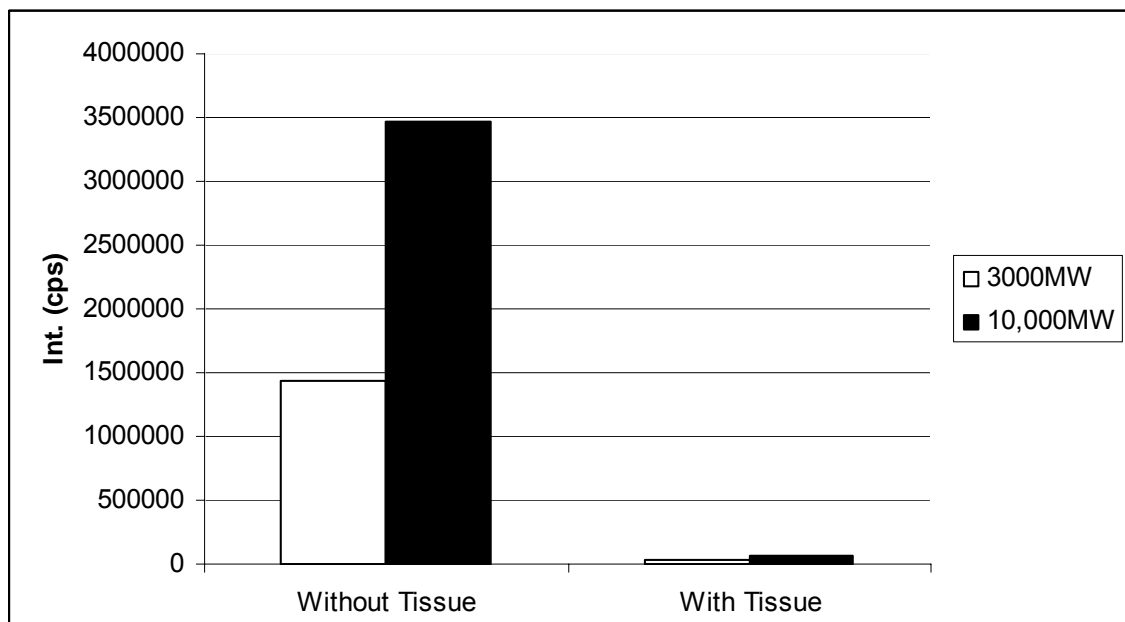


Figure 3.13 Peak Signal from two different probes with tissue and without tissue

There was a drop of 98.2% to the peaks which means only 1.98% transmitted peak signal was captured.

The results from testing different tissue thickness compared to the fluorescence captured showed a drop in the signal as the thickness of the tissue increases, as shown in Figure 3.14.

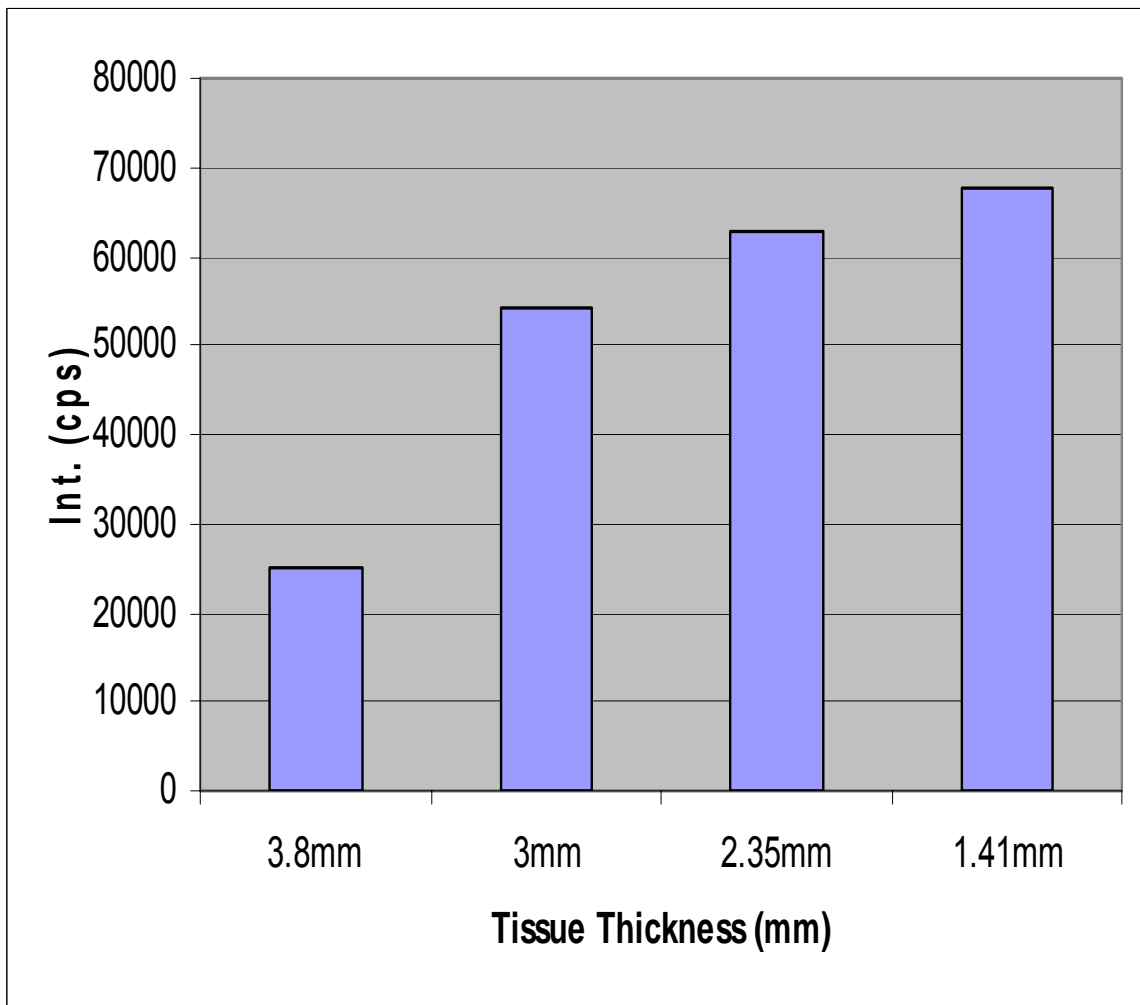


Figure 3.14 The signal from different tissue thicknesses.

When looking at the relation between tissue thickness and the resulting florescence, there is a decrease in the signal as the tissue thickness increases.

As shown in Figure 3.15, this relation is described by the following equation:

$$y = -10045 X^2 + 34922 X + 37998$$

The R^2 value was 0.9926.

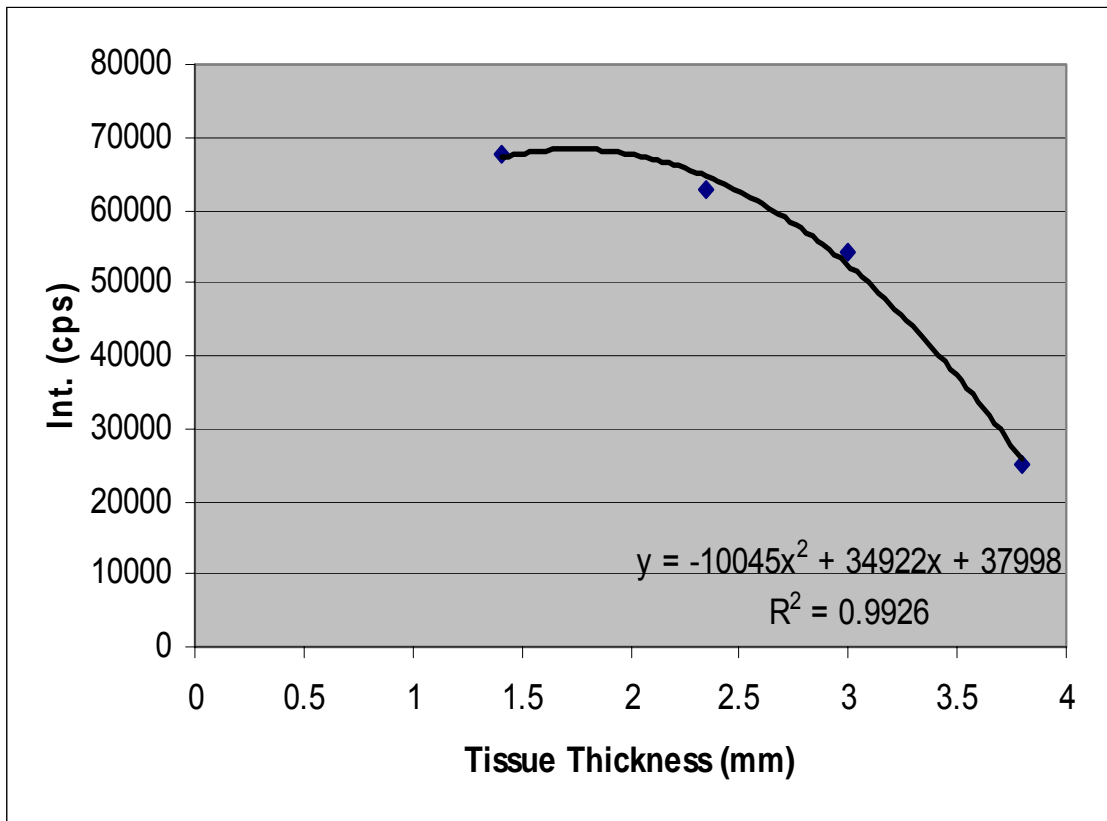


Figure 3.14 Relation between tissue thickness and intensity

These results imparted some important information and will be useful in the final *in vivo* nanoprobe design. The placement of the light source and detector will be extremely important. These components need to be placed in a

location where the skin thickness is minimal. The light source should be powerful enough to penetrate the skin and elicit a strong fluorescence response or else longer wavelength FRET pairs are needed.

3.4 CONCLUSION

FRET is a ratiometric optical technique. It can be utilized as a chemical transduction system to detect glucose. By using NIR FRET pairs in glucose sensing, it allows the idea of *in vivo* glucose sensing feasible, and avoids complete quenching of the signal from blood and tissues. These experiments provided fulfillment of most of the necessary FRET conditions for the AF750 and AF680 as a FRET pair. By exploiting the high affinity between biotin and streptavidin, testing the two dyes was feasible and provided the proximity within the Förster distance, which resulted in FRET. The optimization of the energy transfer was achieved by utilizing different concentrations of the labeled biotin and streptavidin.

The above FRET dye pair was used in testing the effect of dextran size on energy transfer when dextran was bound to Con A. Labeled Con A and dextran were used in detecting glucose optically. Since FRET is a distance dependent technique, the size of the labeled dextran will have an effect on the binding between Con A and dextran. The test on dextran size revealed that Dextran (3000 MW) gave the best results. Also the detection range was adjusted to cover

the upper limit of the normal blood glucose concentration in humans, which is 25mM.

Finally, detecting of peak signal through 4.06mm thick tissue was possible but only 1.92% of that intensity captured. If the tissue thickness is reduced then the captured signal will increase. All the above results can be used in designing more sensitive optical glucose biosensor. These sensors may eventually be deployed for *in vivo* glucose sensing with superior sensitivity and without the concern of toxicity.

CHAPTER 4

NOVEL GLUCOSE NANOPROBES

4.1 Glucose Binding Protein as a Novel Optical Glucose Nanobiosensor

4.1.1 Introduction

In vivo glucose sensing has gained more focus by scientist and researchers, but remained a difficult area due to the number of problems, such as biofouling, poor optical transmission, and poor glucose sensitive probes. There are several enzymes used to detect glucose. But a major problem with these enzymes is the byproduct produced. In the case of glucose oxidase, the hydrogen peroxide will cause major problems with the optical dyes that are pH sensitive. To overcome this problem, Glucose Binding Protein (GBP) will be used to detect glucose. In this research project the GBP structure provides a glucose binding site in a shape of a pocket. When glucose is introduced, it will bind to the glucose binding sites and will cause a conformational change.

The glucose binding protein of *Escherichia coli* (*E. coli*) is considered as an initial component for both chemotaxis towards glucose and high-affinity active transport of sugar. *E. coli* is a bacterial periplasmic binding protein. It is an essential component that serves as initial receptor for active transport systems [67-69]. The X-ray structures of this protein have provided a molecular view of the sugar-binding site and of the site for interacting with the Trg transmembrane

signal transducer [70-73]. Figure 4.1 provides a schematic of the geometry of the sugar-binding site. It is located in the cleft between the two lobes of the bilobate protein. It is designed for tight binding and sequestering of either the alpha or beta anomer of the D-stereoisomer of the 4-epimers galactose and glucose [74]. The diameter of glucose binding protein (GBP) is 50 Å [75].

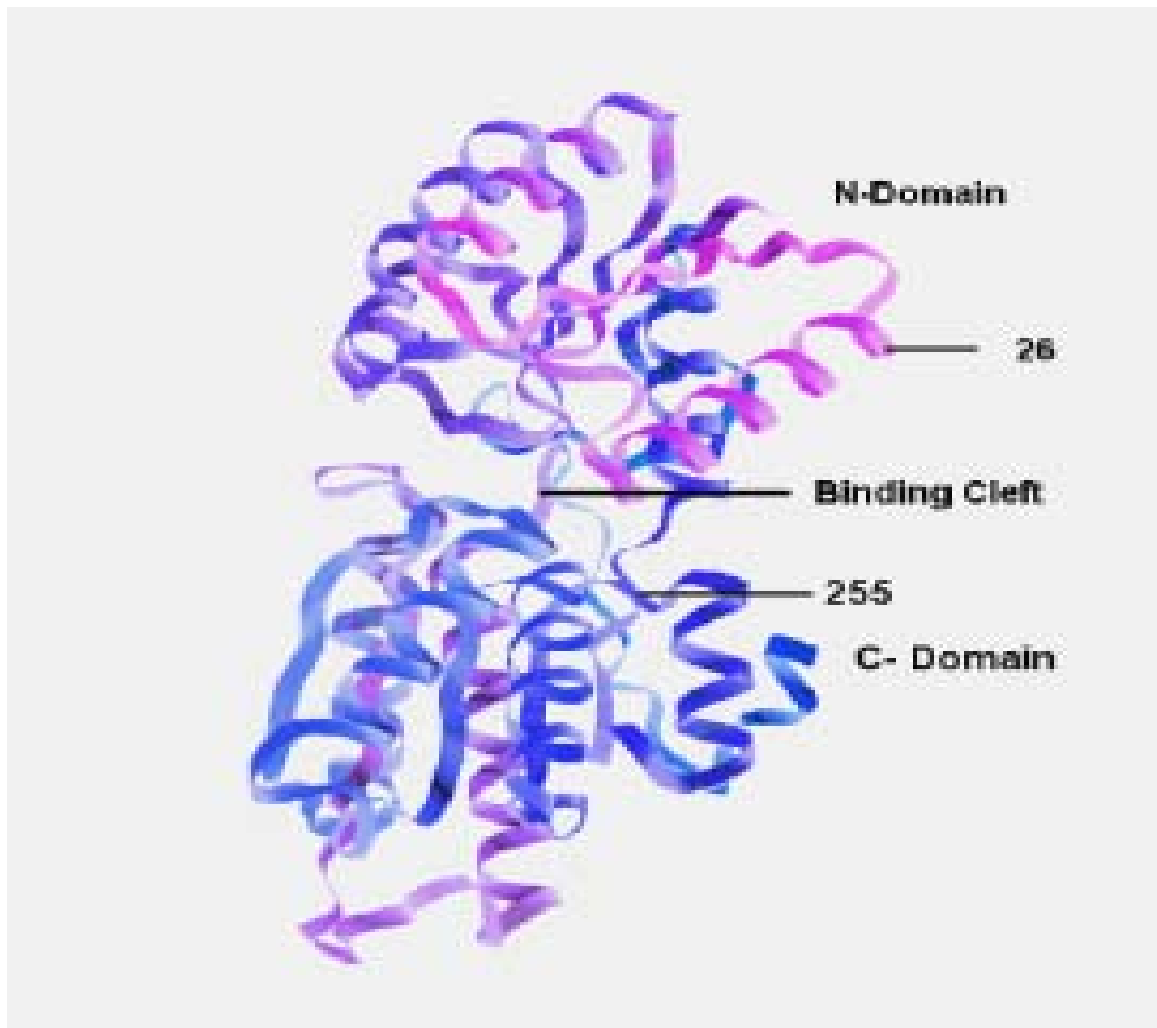


Figure 4.1 schematic of the geometry of the glucose-binding site [76]

Mature GBP consists of 309 amino acids with a molecular weight of 33,310 Da [77]. It is ellipsoidal in shape with two different but similarly folded domains connected by three different peptide segments that serve as a flexible hinge and produce a cleft between the two folded domains. The ligand-binding site is deep within this cleft. Each domain has a core of six β -sheet strands flanked by two or three helices on both sides [78]. In the absence of D-glucose, the two domains remain far apart with the cleft accessible to solvent. Glucose induces a hinge motion in GBP and the sugar becomes completely engulfed in the deep cleft between the two domains. This conformational change in GBP results in the exclusion of solvent molecules from the binding site and enables efficient hydrogen-bonding interactions between the sugar and the residues in the binding site. D-glucose binds to GBP with dissociation constants, K_d , of 0.4 mM [79]. The conformational change produced in GBP upon binding glucose constitutes the basis of FRET nanobiosensor development strategy.

AF750 and AF680 is a viable FRET pair that will be used to label the GBP. Wild-type *E. coli* GBP has multi sites of amino but no cysteine moieties. By incorporating a unique cysteine to the protein, this will permit site-specific labeling with fluorophore and the optimization of the induced fluorescence change in the presence of glucose.

Site-directed mutagenesis was performed to incorporate a single cysteine in GBP at site 175 to produce GBP mutant. This site was chosen because the crystal structure of GBP [80] shows that these residues are located near the

binding cleft. The response of this labeled mutant GBP upon binding with sugar was monitored by following the changes in the fluorescence intensity of the probes. Calibration plots were then constructed by relating the changes in signal with the amount of ligand present.

4.1.2 Materials and Methods

Materials

Glucose binding protein from *E.Coli* that contains a unique cysteine at position 175 was purchased from Senseomics (Lexington, KY). Dithiothceitol (DTT) was purchased from Sigma Chemical Co. (St. Louis, MO). β -D-Glucose and PBS also were purchased from Sigma Chemical Co. (St. Louis, MO). Alexa Fluor 750 C5-maleimide, which was used to label the unique cysteine on the GBP, was obtained from Invitrogen. The Alexa Fluor 680 caboxylic acid, succinmidyle ester was also purchased from Invitrogen. DMSO 78.13 MW was obtained from the MU Chemical Recycling (Columbia, MO). Dialysis tubing 6000-8000 MWCO was obtained from Fisher Scientific (Fairlawn, NJ).

Instrumentation

A UV-Vis absorbance spectrometer (Beckman DU 520) was used to collect absorbance spectra. The slit size (4 nm) and scanning speed (595nm/min) were held constant throughout all the experiments. A scanning fluorescence spectrometer (FluoroMax-3 Jobin Yvon, Hobira) was used to collect

fluorescence emission spectra by exciting the sample at 680 nm. The slit size and integration time were 7nm and 0.3s, respectively.

GBP purifying

The GBP was mixed in Tris-HCl buffer. The addition of Dithiothreitol (DTT) to the GBP was carried out to reduce the disulfide bonds in the GBP. This was accomplished by making a 1 M solution of DTT and then adding GBP. Then the solution was dialyzed in PBS to eliminate the excess DTT. With this process the GBP was ready to allow the cysteine site to be conjugated. The labeling of GBP with AF750 was prepared by using the labeling kit protocol from Ivitrogen.

Bio-Rod experiment was conducted to determine the final protein concentration and the degree of labeling. The final GBP-AF750 concentration was 0.8091 mg/ml and the degree of labeling (DOL) was 1 since there was only one cysteine.

AF680 labeling on the GBP amine sites

By following the protein conjugation protocol from Ivitrogen; the AF680 was conjugated on the GBP amino sites. The conjugated stock was dialyzed in PBS to remove the excess AF680. Then the final conjugated GBP concentration was determined by using a Bio-Rod kit. The final concentration was 0.7842 mg/ml. The DOL was calculated according to this formula

$$\text{DOL} = (\text{A max} \times \text{MW}) / ([\text{Protein}] \times \epsilon \text{ dye}) \quad (\text{eqn 4.1})$$

where A_{\max} is the absorbance at the maximum peak of the fluorophore used in conjugation, and ϵ_{dye} is the extinction coefficient at λ_{\max} in $\text{cm}^{-1}\text{M}^{-1}$, and $[M]$ is the molarity of the agent. MW is the molecular weight of the protein. The DOL was 1.5, which means that for every mole of protein there was 1.5 moles of dye.

The existence of AF 680 and AF 750 on the GBP

Experiments were conducted in 2 ml total volume of PBS. First, 11.32 ug of GBP-AF750 was placed in the 4 ml cuvette. It was scanned for background signal of the AF750. The excitation was set at 750 nm with slit opening at 5. The increment was set at 1 nm and the integration time was at 0.3 sec. Second, 11.32 ug of GBP-AF680-AF750 was placed in the 4 ml cuvette with 2 ml PBS. The scanning fluorescence spectrometer was adjusted to conduct the experiment according to the fluorophore used. The excitation was set at 680 nm, which was the excitation wavelength for the AF680 located on the amine sites. The increment was set at 1 nm and the integration time was at 0.3 sec.

Baseline scan from the FRET pair labeled GBP

It is imperative to establish baseline scans from the FRET labeled GBP. The baselines provide background spectra prior to the addition of glucose.

Glucose Response Experiments

After 2 hr incubation of the 1.56 μg of labeled GBP in PBS buffer probe samples were tested for glucose response. The tests consisted of six additions of

glucose concentrations, 0 to 60 μ M. For each glucose addition, 5 min. was allowed for incubation at room temperature. Calibration plots were obtained by relating the average fluorescence change with the concentration of glucose in the sample. The data points shown in the figures are the average of three measurements ± 1 SD.

4.1.3 Results and Discussion

GBP Labeling and Fluorescence Resonance Energy Transfer (FRET)

Experiments

Figure 4.2 indicates a successful labeling of the AF750 on the one cysteine site and AF680 on the amino sites. When GBP-AF680 was excited at 680 nm, an emission peak signal was detected at 702 nm. After the labeling of AF750, the labeled GBP with AF680 and AF750 was excited at 680 nm. There were two emission peaks. One peak was at 702 nm, which is an indication of the presence of AF680, and another peak was at 776 nm, which is an indication of the presence AF750.

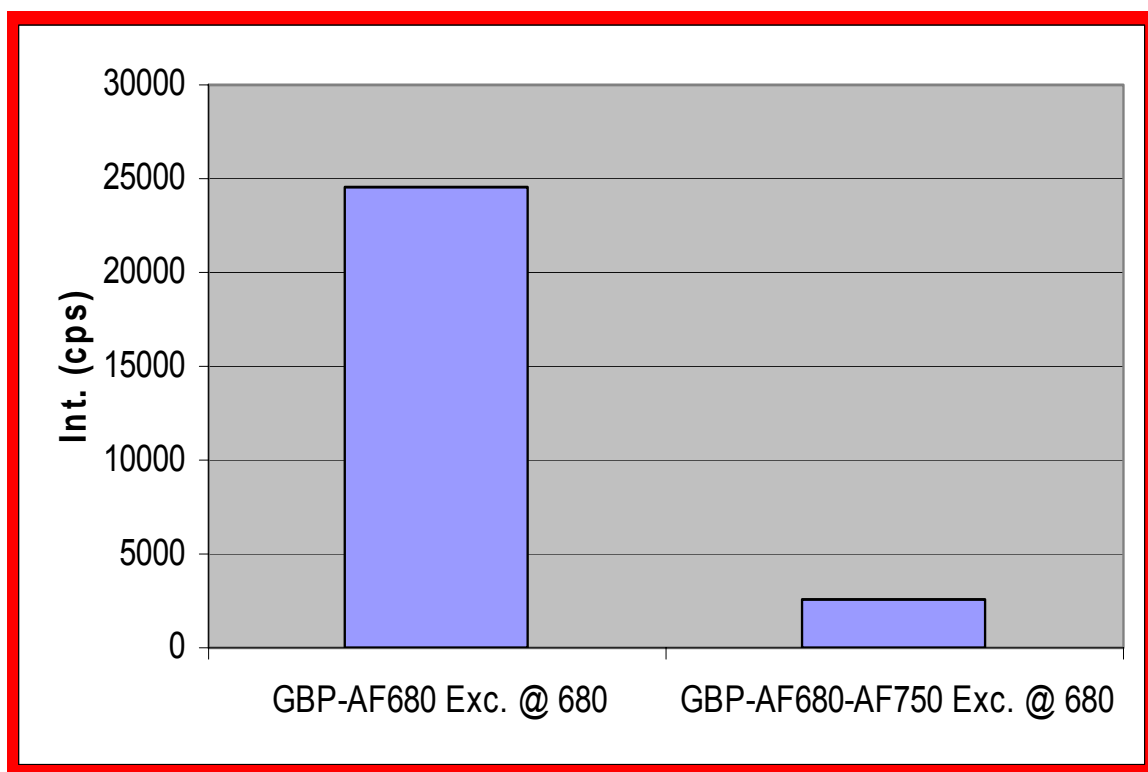


Figure 4.2. Background signal of the labeld GBP-AF750-AF680

The successful labeling of GBP with the NIR FRET dye pair will allow us to quantify FRET results after exposure to glucose. When the GBP was first labeled with the donor, AF680, a scan of GBP-AF680 in PBS was obtained. The maximum peak from the AF680 without the presence of the donor was 24480 CPS as shown in Figure 4.3. The labeled GBP with AF680 and AF750 was scanned, the donor peak result was 2610. Both peaks of AF680 without the presence of the acceptor and with the presence of the acceptor was used to quantify the energy transfer that took occurred between the donor and the acceptor prior to glucose additions.

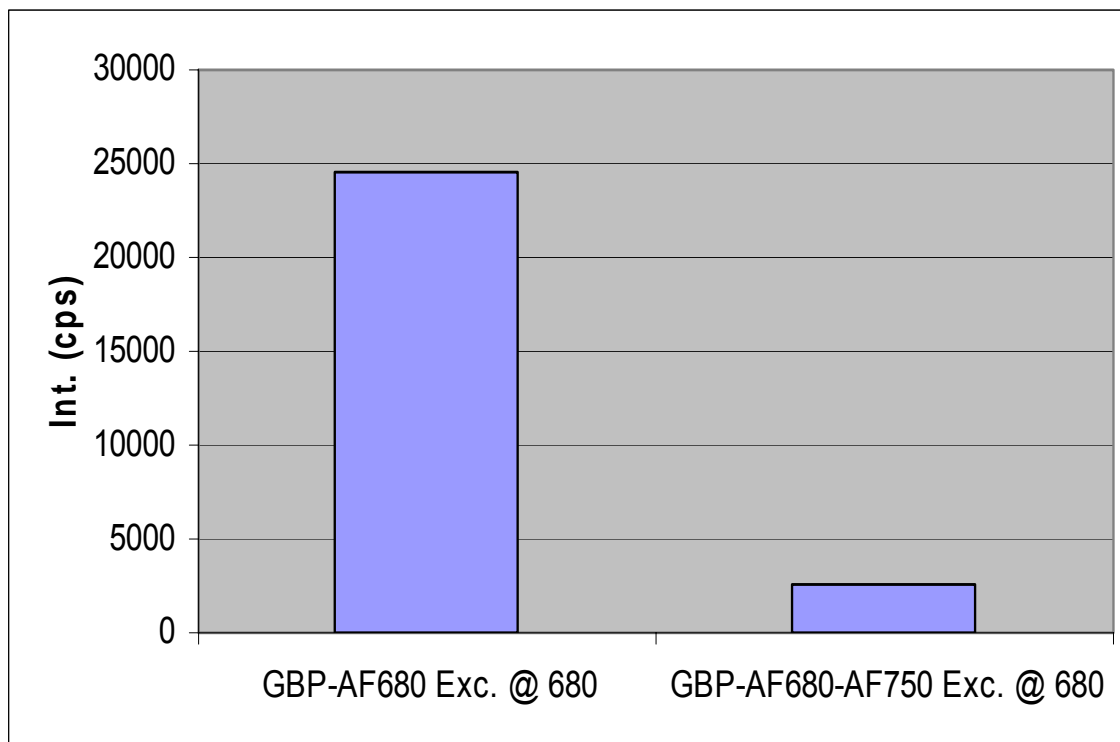


Figure 4.3. Donor peaks at 702 nm with and without acceptor presence

Equation 4.2 was used in the quantification.

$$\% \text{ Energy transfer} = 1 - I_{\text{DWA}} / I_{\text{D}} \quad (\text{eqn 4.2})$$

where I_{D} is the donor's intensity without acceptor and I_{DWA} is the donor's intensity with acceptor present. The result indicated an energy transfer of 89.34%. These results provided conclusive observations of energy transfer in terms of an increase in the acceptor peak and decrease in the donor peak prior to glucose additions.

GBP Glucose Response Experiments

Since it was determined that the AF680 and AF750 fluorophores were labeled to the GBP, the next step was to utilize the fluorophores in a FRET-based glucose biosensor. In these experiments glucose response was studied by utilizing 1.56 μg of GBP-AF750-AF680 in 2ml PBS as a baseline and adding various concentrations of glucose.

The labeled GBP was incubated in the PBS for 2 hours in PBS. Then three different D-glucose concentrations were added: 10 μM , 40 μM , and 120 μM . The scanned data was plotted as donor/acceptor (D/A) ratio vs. glucose concentrations. As shown in Figure 4.4, there was an exponential decrease to the ratio as glucose concentration was increased. This change in the signal is due to the conformational changes of the GBP. As glucose binds to its GBP binding site, the distance between the labeled sites was changed. The results of the increase in the acceptor peak and decrease of the donor peak indicated a decrease in the distance between the donor and the acceptor, resulting in an increased in energy transfer.

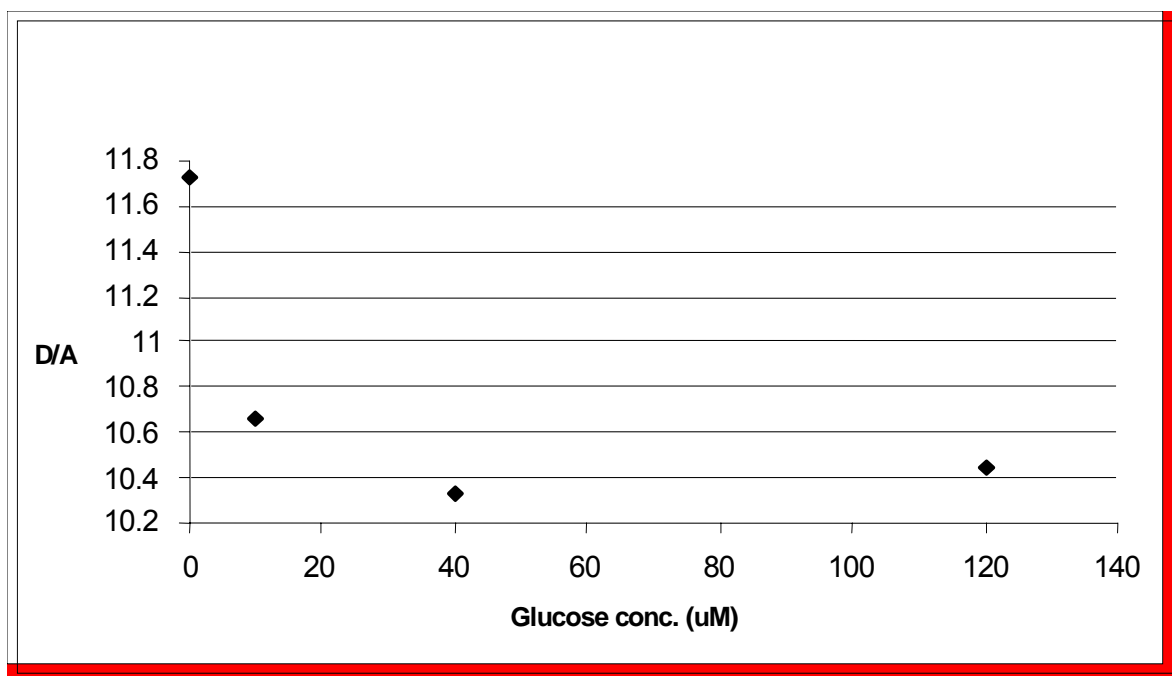


Figure 4.4. D/A vs. glucose concentration (detection range 0 to 120uM)

At 120 uM glucose, the D/A ratio was not consistent with the other two D/A ratios. That result was further investigated by looking into the detection range for the labeled GBP.

A smaller dynamic range of the glucose concentration was tested from 0 to 60 uM. Figure 4.5 provided a consistent decrease in sensor response as the glucose concentration was increased.

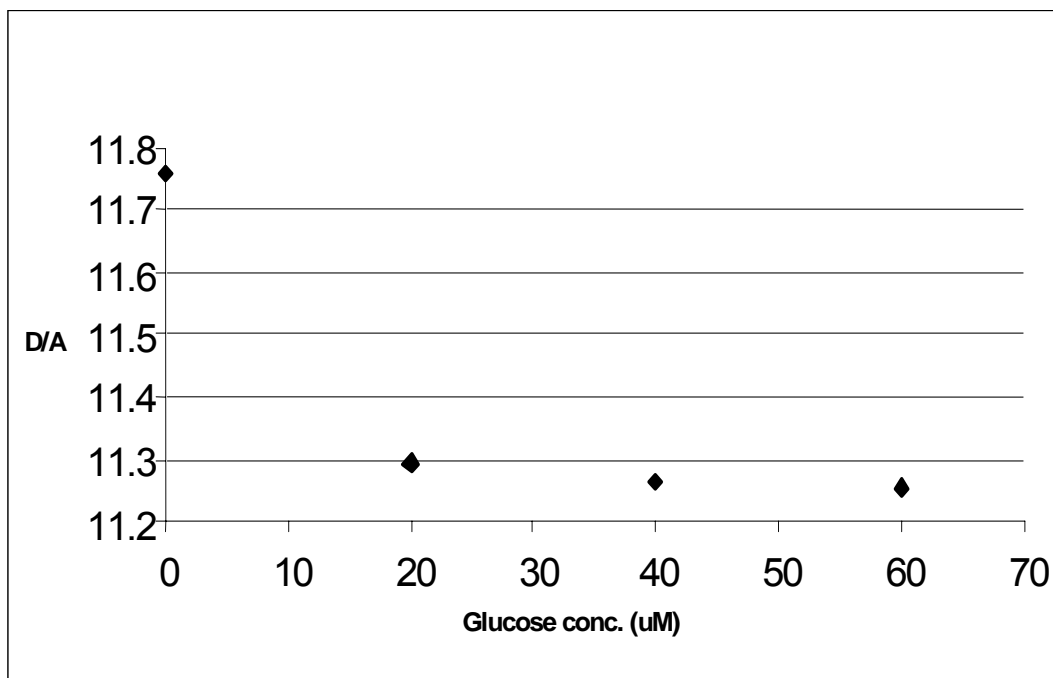


Figure 4.5. D/A vs. glucose concentration (detection range 0 to 60uM)

The final experiments were to target improvements in the signal by modifying the labeling process. In the following section, the ratio of mole dye/mole protein was about 3.6:1. We had 8.7 pmole of dye to every 2.38 pmole of protein. There were more glucose concentration additions within the same tested range of 0 to 60 uM.

Glucose response was also studied at $t=0$ min. and $t = 5$ min. At $t=0$ min., the scan of the sample was performed immediately after mixing. No time was allowed for incubation. The result still showed an exponential decrease to the D/A ratio as the glucose concentration increase as shown in Figure 4.6.

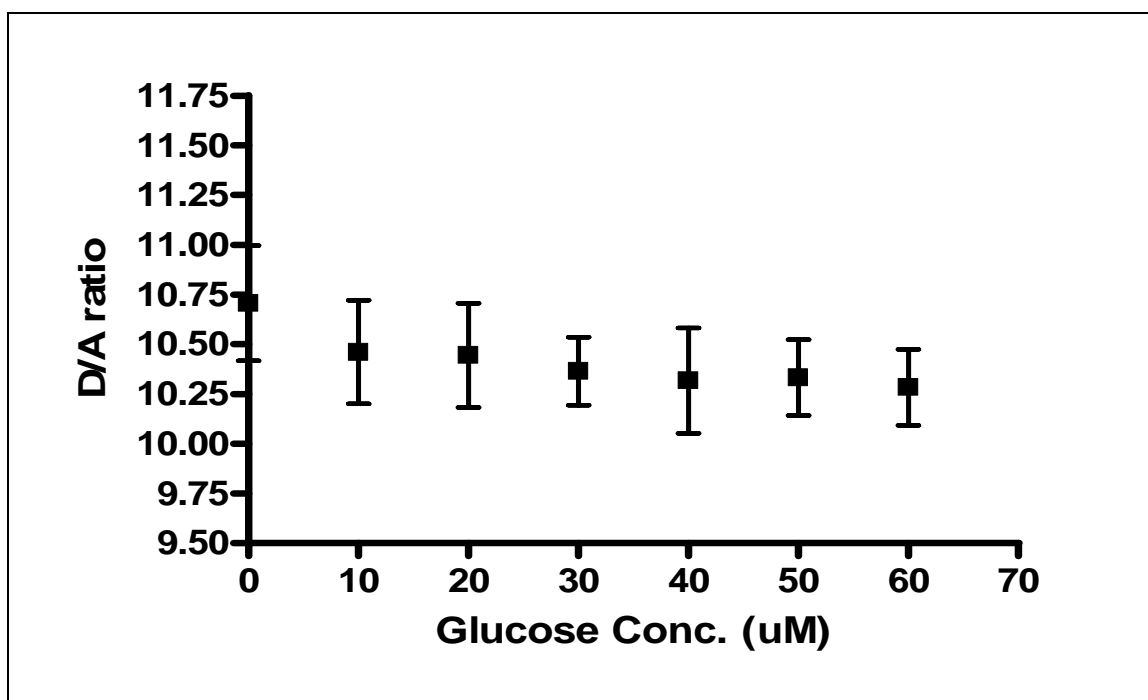


Figure 4.6. Glucose response to different samples at t=0min.

Figure 4.6 show the final graph all three experiments. This result is represented by the following exponential equation was obtained.

$$Y = 10.43 e^{-0.0006 x}$$

The R^2 value is 0.8583

At $t = 5\text{min.}$, the D/A ratio was more consistent in the exponential decrease as the glucose concentration was increasing as shown in Figure 4.7.

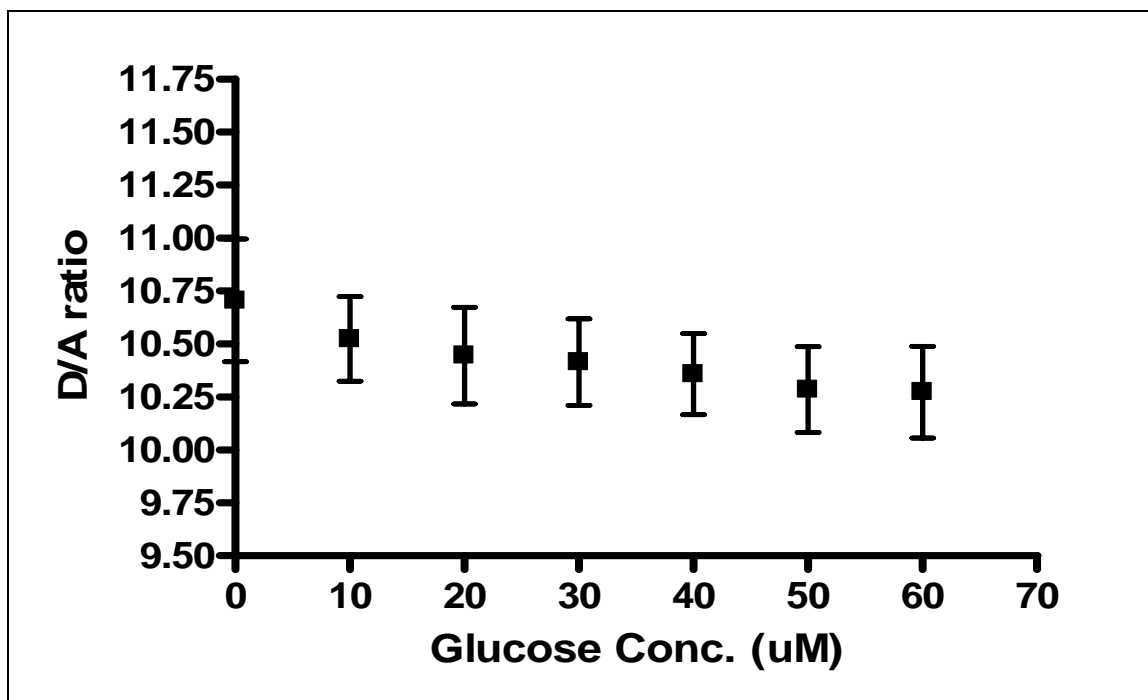


Figure 4.7 Glucose response of three samples at t=5min

Figure 4.7 show the final graph all three experiments. By using Figure 4.7, we got the following exponential equation was obtained.

$$Y = 10.391e^{-0.0005 x}$$

The R^2 value is 0.7317.

It is conclusive that incubation time is very important after the addition of different glucose concentrations.

4.1.4 Conclusion

Glucose binding protein (GBP) is a monomeric periplasmic protein. It binds glucose with high affinity. The binding mechanism is based on a hinge motion due to the protein conformational change. This change was used as an optical sensing mechanism by applying Fluorescence Resonance Energy Transfer (FRET). With the introduction of a single cysteine at a specific site by site-directed mutagenesis, a single-label attachment at specific sites with a fluorescent probe, AF750, was ensured. The other sites are amino sites, which were labeled with a donor fluorophore, AF680. Since this residue was not involved in ligand binding and since it was located at the edge of the binding cleft, it experienced a significant change in environment upon binding of glucose. The sensing system strategy was based on the fluorescence changes of the probe as the protein undergoes a structural change on binding. This structure change allowed a reduction in the distance between the donor and the acceptor, which allowed more energy transfer as glucose concentration was increasing. Also by allowing 5 min for glucose to incubate, the respond from the biosensor was decreasing exponentially as glucose concentration was increasing. The detection range was determined between 0-60 μM . The dynamic range could be improved by increasing the GBP concentration.

All the above results can be used in designing more sensitive optical glucose biosensor. These sensors may eventually be deployed for *in vivo* glucose sensing with superior sensitivity and without the concern of toxicity.

CHAPTER 5

NANOPROBES ENCAPSULATION IN ERYTHROCYTES

5.1 Encapsulation of Streptavidin labeled with Alexa Fluor 750 into Erythrocytes

5.1.1 Introduction

An essential task of erythrocytes, (Red Blood Cells, RBCs) is to carry oxygen to different body tissues. RBCs are biconcave disks, which allow maximum oxygen transport. There are 5-million/micro liters of RBCs in the circulation (totaling 30 trillion in humans), and they have long lifetimes of 120 days [81]. Figure 5.1 details the shape and dimensions of RBCs.

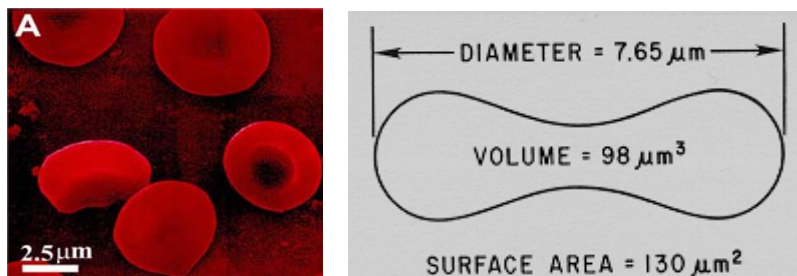


Figure 5.1 An SEM image of red blood cell. The cells were obtained from rabbits [82]

Erythrocytes have remarkable capacity to undergo reversible membrane swelling. This flexibility in the membrane allows large pores to open up where metabolites and macromolecules can cross that barrier [83]. For more than 20 years this property has been carefully investigated by a number of different

researchers and laboratories [84] due to the idea of using red cells as storage containers (erythrocyte encapsulation) [85-88]. Encapsulated erythrocytes have been proposed as carriers and bioreactors, which would be suitable for use in the treatment of various diseases [89-90].

There are several methods currently in use that allow the encapsulation of agents in erythrocytes. They are based on a high-hematocrit dialysis procedure [91]. The procedure for the encapsulation of RBCs starts by placing the washed RBCs in dialysis tubing together with the substance to be encapsulated. The suspension is then dialyzed against a hypotonic solution until the erythrocytes have been lysed. The dialyzed cells, once in equilibrium with the exogenous substance, are resealed by restoring the physiological isotonicity, then washed and resuspended in plasma or in a physiological saline solution as shown in Figure 5.2.

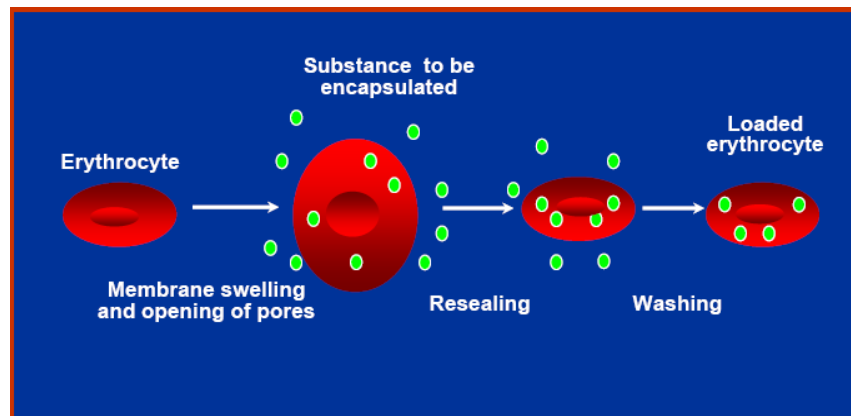


Figure 5.2 Biotechnol. Appl. Biochem. (1998) 28, 1–6 (Printed in Great Britain) 1

Erythrocytes are attractive systems due to their ability to deliver proteins and therapeutic peptides. They have also been used as transport for enzymes destined for the correction of metabolic alterations as L-asparaginase, alcohol dehydrogenase (ADH) and aldehyde dehydrogenase (AIDH) among others.

The overall goal of this project is to utilize RBCs as carriers for biosensors. But first the possibility of loading RBCs with just fluorescence dyes was examined. To determine the loading success of a fluorescence dye, Alexa Fluor 750 was utilized to encapsulate in RBCs. Then we used optical equipment to excite the dye and examine its emission after the loading.

The illustration of the RBCs encapsulation with AF750 is shown in Figure 5.3. The hypo-osmotic dialysis technique was utilized to load the RBCs. The specific objective was to acquire data on:

1. The hypo-osmotic technique with longer emitting fluorophores loaded into red cells to demonstrate signal capture through red cells.
2. Signal acquisition through porcine aorta of longer emitting fluorophores mixed with red cells to demonstrate signal capture through tissue.

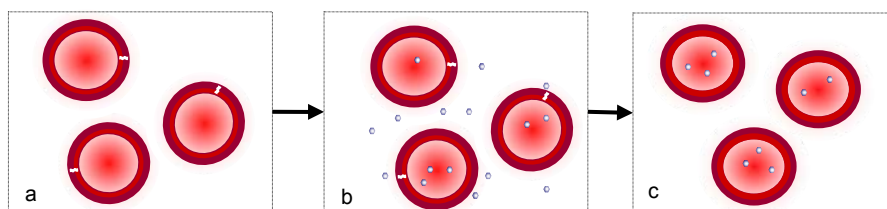


Figure 5.3. Loaded red cell overall design. a) Lyses of the red cell; b) Exposure to nanoprobes; c) Sealed and washed red cell encapsulated nanoprobes.

The results from these experiments will be utilized in designing optical sensors encapsulated in RBCs.

5.1.2 Materials and Methods

Materials

In the experiment 10,000 MWCO slide-a-lyzer cassettes (Cole-Parmer EW-02905-42) were used. 20G needles and 3ml syringes were also utilized. 500 ml phosphate buffer, pH 7.4 was made by using 202.5 ml 200 mM Na_2HPO_4 and 47.5 ml 200 mM Na_2HPO_4 . 1 L of Dialysis buffer was made by using 250 ml phosphate buffer from above added to 36.4 ml of 110 mM MgCl_2 . Alexa Fluor 750 1100 MW, 1mg (Invitrogen – A-20011) was purchased from Invitrogen (Carlsbad, CA). DMSO 78.13 MW (MU Recycling – D-5879 – lot 100F-0269) was obtained from MU Recycling. PBS 0.01 M, pH 7.4 (Sigma - P-3813 - lot 075K8206) was purchased from Sigma. 500 ml BV WH Blood NS Heprin (Pal-Freez Arkansas – 37132-1) was purchased from Pal-Freez.

Instrumentation

The Beckman centrifuge, which spins down and purifies the RBCs from plasma, platelets, and white cells was utilized. Also, a fluorescence spectrometer (FluoroMax-3 Jobin Yvon, Hobira) was used to collect fluorescence emission spectra by exciting the sample at 749 nm. The slit size and integration time were 5 nm and 0.5 s, respectively.

Methods

There are several methods currently available for the encapsulation of macromolecules into erythrocytes [81]. Most of these procedures involve the dialysis of erythrocytes against a hypotonic solution, the addition of the substance to be encapsulated and the resealing of the lysed cells. Other methods are also available (e.g. electroporation, drug-induced endocytosis and the osmotic pulse method) [80] but usually these are best suited for the processing of very small volumes of erythrocytes. The hypo-osmotic dialysis method we have used is based on the following steps:

1. Washed red blood cells (bovine) were mixed with an isotonic solution containing isotonic NaCl and the relevant dyes. In the experiment, the suspension contained 90% cells and 10% dye solution.
2. Two mls of the mixture were placed in a Pierce dialysis slide (MW cut off ~10,000). The slide was placed in a beaker of ice cold solution containing 4 mM MgCl₂, 25 mM Na phosphate, pH 7.4. The incubation time was 30 minutes.
3. During this time, the red blood cells lyse and the contents equilibrate with the solution inside the slide (hemoglobin and dye mix) and the small molecules escape out of the dialysis slide.
4. The dialysis slide was then transferred to a beaker with ice cold 165 mM NaCl, incubated for 30 more minutes on ice during which time the NaCl enters the slide and the cells.

5. Then the slide was transferred to 200 mls of an ice cold solution containing 150 mM NaCl, 10 mM Pi (Na salt) pH 7.4, 5 mM adenosine, 5 mM glucose, 5 mM MgCl₂ and incubated an additional 30 minutes.
6. Then the cells were incubated at 37C for 1 hour to reseal.
7. The red blood cells were then removed from the dialysis slide and washed twice in 165 mM NaCl by centrifuging for 3 minutes at 10,000 rpm. (Note that red blood cells do not need to be in a buffered solution because of the high buffer capacity of hemoglobin and the robust pH equilibration via the anion exchanger).

With the completion of loading the RBCs, they were ready to scan. The loaded cells were placed in a cuvette with buffer. The cuvette will be scanned in the spectrometer. The excitation was set at 750nm with slits size 5.

We have utilized the hypo-osmotic dialysis technique to successfully make “ghosts” that were loaded with the fluorophore, AF750. After encapsulation, the red cell solution was placed in 1.26 mm (inner diameter) tygon tubing. A special holder was machined to hold the tube in an ISA spectrofluorometer. The fluorescence or absorbance spectra of the cell pellets was then determined.

5.1.3 Results and Discussion

The objective was to demonstrate the ability to capture fluorescence from fluorophore-encapsulated red cells.

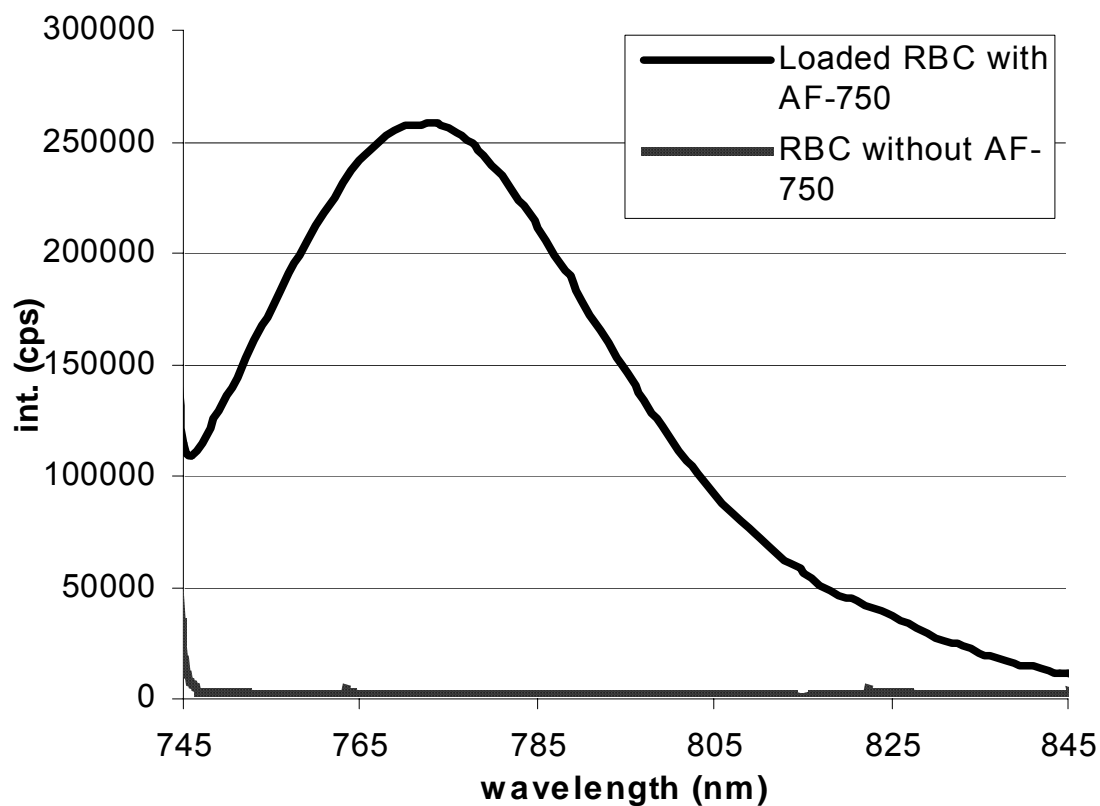


Figure 5.5. Fluorescence signal acquisition of AF750 dye loaded into red cells.

Figure 5.5 displays fluorescence spectra of the cells loaded with AF750. Hemoglobin absorbance at ~ 800 nm is 200 liter/mol \cdot cm. AF750 is 250,000 liter/mol \cdot cm. Thus, AF750 has ~ 1000 times greater absorption and we see a strong fluorescence peak at ~ 770 nm. The volume of the dye in the red cells was ~ 10 μ m.

The graph demonstrated the success of the loading procedure and our ability to measure dye fluorescence even in the presence of hemoglobin.

5.2 Encapsulation of Streptavidin labeled with Alexa Fluor 680 and BSA labeled with Alexa Fluor 750 into Erythrocytes

5.2.1 Method

We will use the same method of encapsulation of macromolecules into erythrocytes as we did in the previous experiment. The procedure involves the dialysis of erythrocytes against a hypotonic solution, the addition of the substance to be encapsulated and the resealing of the lysed cells. This method allowed maximum loading technique.

There is a large number of RBCs, 5 million/ul. This number of cells will be used to estimate the number of loaded cells after the encapsulation. The volume of a RBC is 179.5 femto liters (fl). The 5 million cells will require 0.8975ul of probes to load.

In this experiment, the RBCs will be loaded with SA-AF680 and BSA-AF750. The objective is to detect a FRET signal of the bound SA-AF680 and BSA-AF750. There will be three different samples of packed cells to load.

- a. Sample 1 has about 500 (million) RBCs. The probe volume will be 18ul of bound SA-AF680 and BSA-AF750.
- b. Sample 2 has about 1100 (million) RBCs. The probe volume will be 180ul of bound SA-AF680 and BSA-AF750.

- c. Sample 3 has about 30,000 (million) RBCs. The probe volume will be 36ul of bound SA-AF680 and BSA-AF750.

The loaded cells will be scanned after the dialysis. The first scan will be the supernatant and then will scan the final sample after several washes.

5.2.2 Results and Discussion

The Detection of signal from loaded RBCs was performed by placing each sample in 1ml cuvette and then scans. The spectrometer was set to excite at 680nm with slits open to 5. The integration time was 0.3s.

Sample 1 was scanned several times. Figure 5.7 Show a clear signal of the donor, SA-AF680, and the acceptor, BSA-AF750. This sample was taken after the first wash, which called supernatant 1.

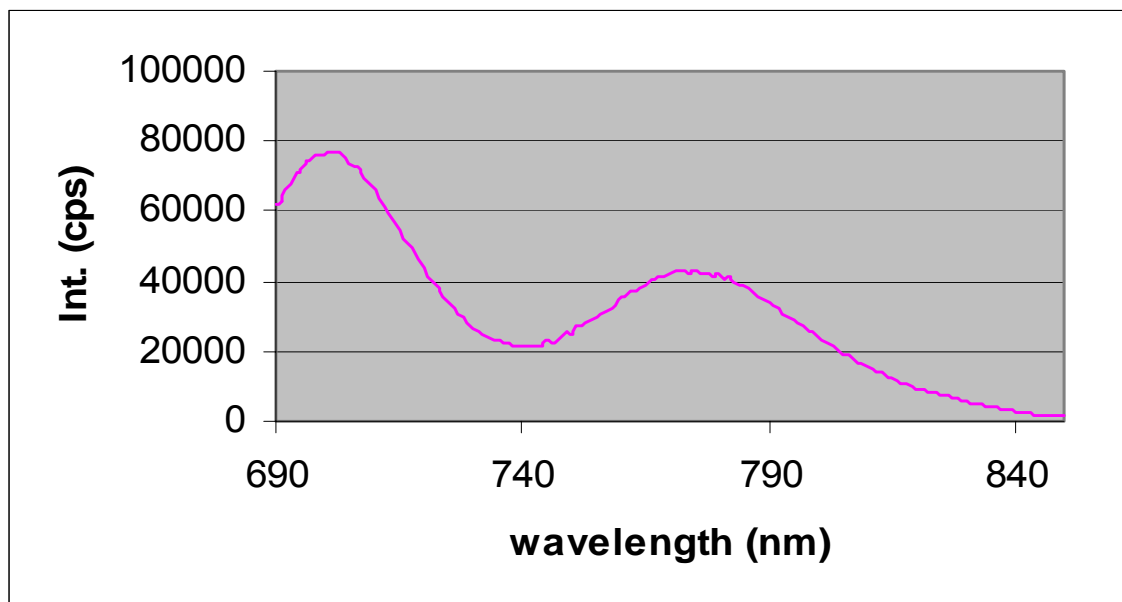


Figure 5.7 Scan of supernatant 1 from sample 1

When the loaded RBCs were separated, then they were scanned in a buffer, the signal on both the donor and the acceptor was reduced (figure 5.8).

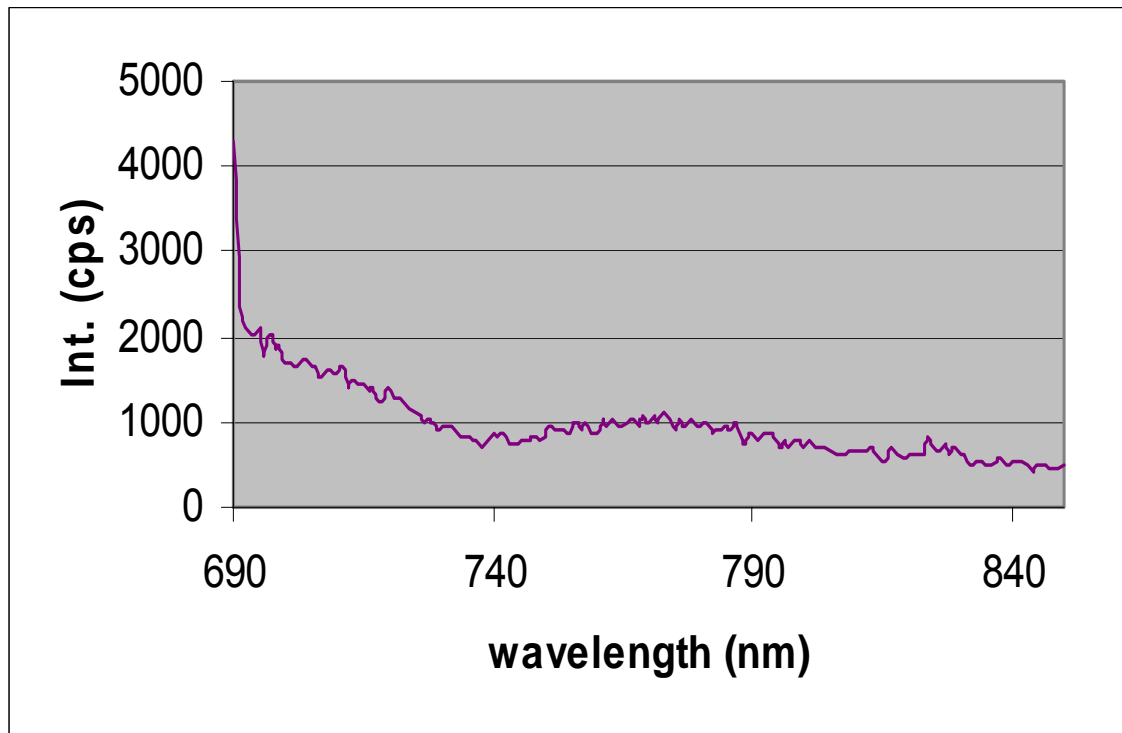


Figure 5.8 Scan of loaded cells in buffer

This drop of about 97% in peak signal is due to the low number of loaded cells.

Sample 2 showed better results than sample 1. This was due to the large number of the loaded cells. In this sample there were about 1100 (million) RBCs which require about 197.45ul of probes. The total volume of probes used was 180ul. Those numbers indicated that an estimated 91.16% of the cells were loaded with probes, whereas in sample 1, there were about 20.06% of the cells

loaded. Figure 5.9 show both scans of the supernatant and the loaded cells in buffer.

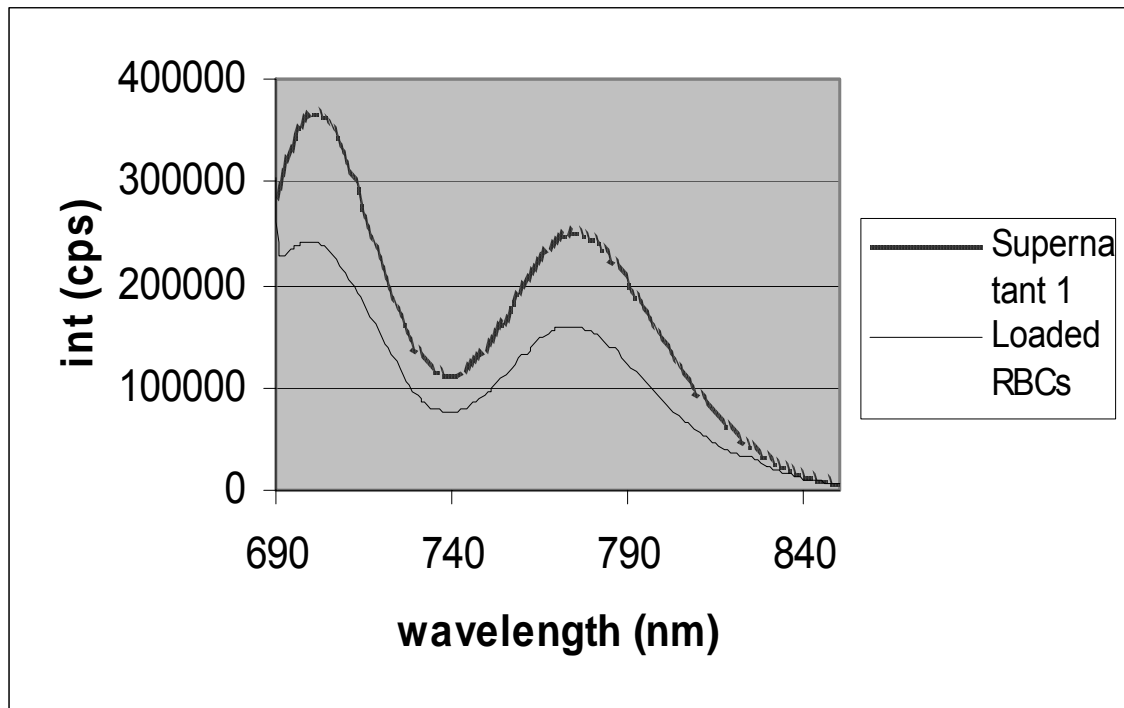


Figure 5.9 Scans of supernatant and loaded cells in buffer

Sample 3 provided a very low percentage of loaded cells. There were only 0.67% of the cells loaded. Figure 5.10 shows an indication of the existence of the probes. This was a scan of the supernatant 1. But when the cells were placed in buffer after the last wash, there was no signal (Figure 5.11).

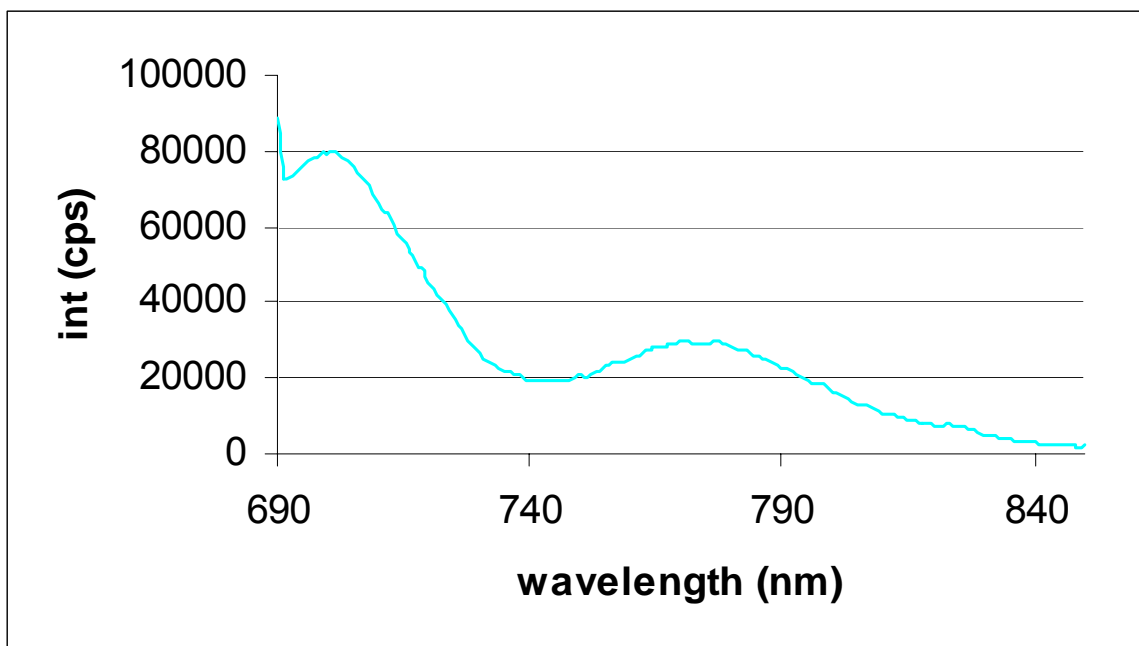


Figure 5.10 Scan of supernatant 1 for sample 3

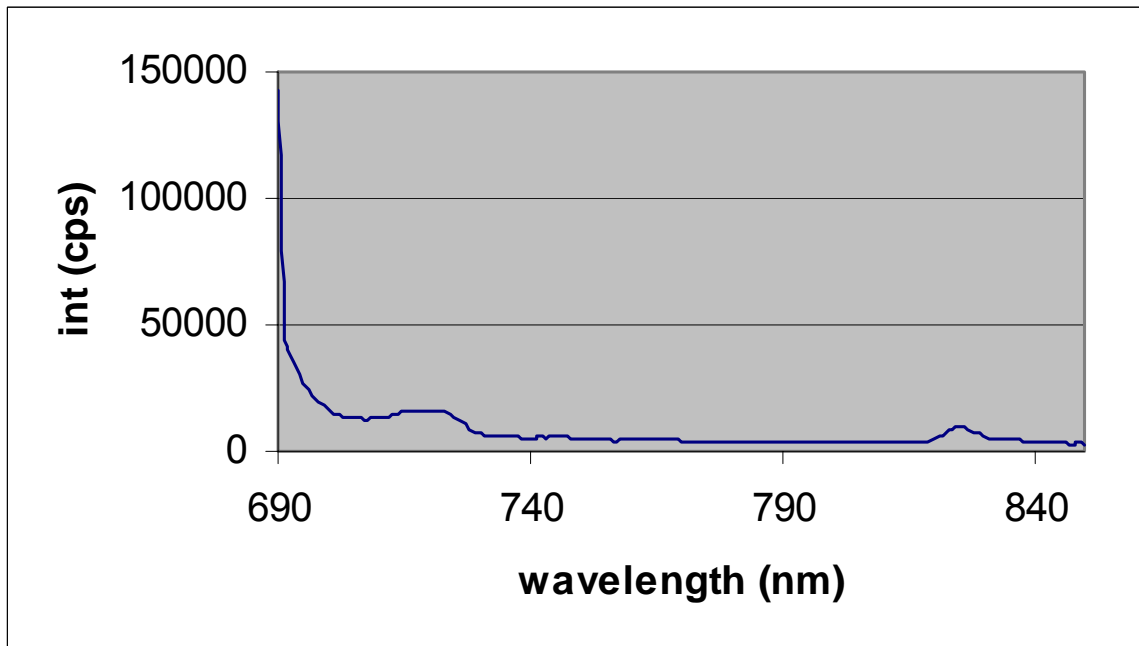


Figure 5.11 Scan of the loaded cells in buffer

It is conclusive that sample 2 showed the best results and provided the best signal. These results will be used in reaching consistency and repeatability in the loading process.

5.3 Signal Detection of NIR Fluorescence Encapsulated Erythrocytes through Tissue

5.3.1 Method

We will use the same method of encapsulation of macromolecules into erythrocytes as we did in the previous experiment. The procedure involves the dialysis of erythrocytes against a hypotonic solution, the addition of the substance to be encapsulated and the resealing of the lysed cells. This method allowed for the maximum loading technique.

With the completion of loading the RBCs, they are ready now to be scanned. The loaded cells will be placed in a cuvette with buffer. The cuvette will be wrapped with porcine aorta tissue that has a thickness of 2.26 mm. This experiment will mimic the ability to detect a signal from a loaded cell through a tissue. The spectrometer will be used to scan sample. The excitation will be set at 750nm with slits size 5.

5.3.2 Results and Discussion

The objective from this experiment is to determine if fluorescence from AF750 (1 μ M or 10 μ M) in red blood cell solution can be captured through porcine aorta tissue. The loaded RBCs are placed in a 1ml cuvette. Then they

will be flowing through 1.26 mm tygon tubing. This tubing runs through a holder, which it wrapped with a porcine aorta (figure 5.12).

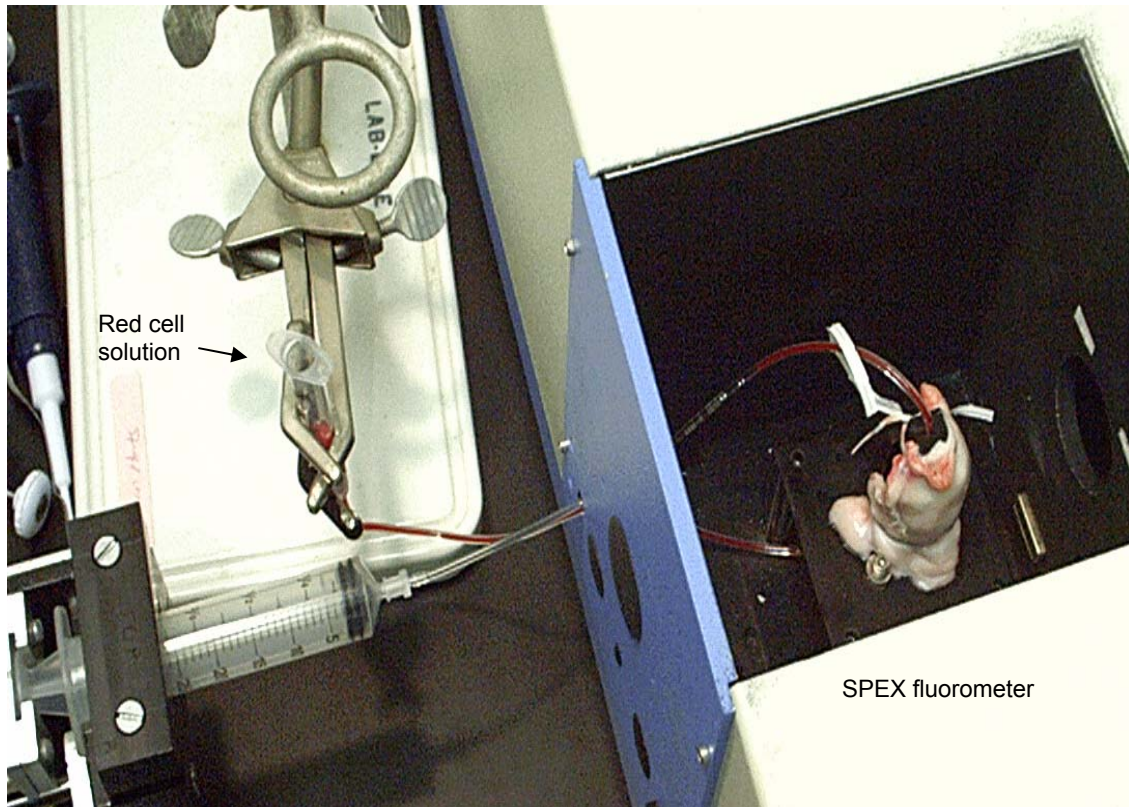


Figure 5.12 Set up of the tissue wrapped

We have utilized the hypo-osmotic dialysis technique to successfully make “ghosts” that were loaded with the fluorophore, AF750. After encapsulation, the red cell solution was placed in 1.26 mm (inner diameter) tygon tubing. A special holder was machined to hold the tube in an ISA spectrofluorometer. The fluorescence or absorbance spectra of the cell pellets were then determined. Figure 5.13 displays fluorescence spectra of the cells loaded with AF750.

Hemoglobin absorbance at ~800 nm is 200 liter/mol·cm. AF750 is 250,000 liter/mol·cm. Thus, AF750 has ~1000 times greater absorption and we see a strong fluorescence peak at ~770 nm. The volume of the dye in the red cells was ~10 μ m.

The graph of Figure 5.13 demonstrated the success of the loading procedure and our ability to measure dye fluorescence even in the presence of hemoglobin.

Bovine red cell solution with and without AF750 was placed in a 1.26 mm (inner diameter) tygon tubing. Again, the special holder was utilized to hold the tube in the spectrofluorometer. Next, an aorta ~2.26 mm thick (porcine) was wrapped around the tube holder as shown in Figure 5.12. Fluorescence scans were acquired of the blood + tissue wrap + 1 μ M (or 10 μ M) AF750 after subtraction of the background.

Also Figure 5.13 displays the intensity scans. At a 10 μ M concentration of AF750, there is a large fluorescence peak captured through the tissues. And, there is a distinguishable peak with the lower concentrations of dye, above that of the red blood cell solution.

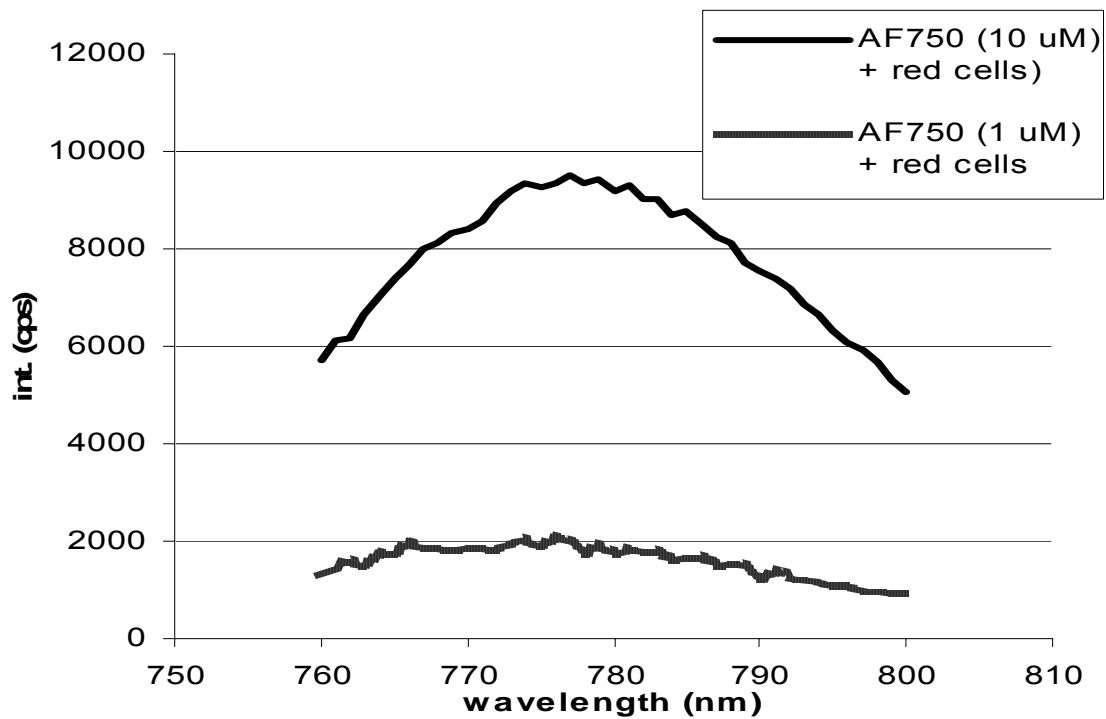


Figure 5.13 Fluorescence signal capture of AF750 dye through a porcine aorta.

It is possible to capture the fluorescence from AF750 not only at 10 uM, but also 1 uM when encapsulated in red blood cells and passed through porcine aorta tissue. These results will be use to further pursue a more sensitive detection system.

5.3.3 Conclusion

This experiment provided important finding. They hypo-osmotic technique was a good method for loading the RBCs. NIR fluorescence dye is very important long wave dye, which could be excited, and its signal detected through all the substances in the RBCs.

This paper provided a good and important finding. The encapsulation of RBCs with fluorophore is possible. This finding could be used in developing optical sensors for detecting several analytes. One of which is glucose. By using Fluorescence Resonance Energy Transfer (FRET) for glucose sensing that will allow the idea of in vivo glucose sensing without worrying about the signal interference of the blood. These sensors may eventually be deployed for in vivo glucose sensing with superior sensitivity and without the concern of toxicity.

In this experiment, we took it to a further step by wrapping the cuvette with a 2.26 mm porcine aorta tissue. Successfully, a signal was detected from that setup. This setup is a simulation of loaded RBCs in a body and the aorta is the skin barrier.

The success of capturing the fluorescence from AF750 at not only 10 μM , but also 1 μM when mixed in a red blood cell solution and passed through porcine aorta tissue, will allow further work toward the development of implantable sensor. These results also let us work on more sensitive detection system.

CHAPTER 6

SUMMARY AND FUTURE WORK

The development of a novel glucose biosensor was successfully achieved. This FRET-based biosensor has shown detection sensitivity in the micromolar.

The main objective was to utilize NIR FRET pairs in order to label GBP and other proteins so that we can detect changes in blood glucose concentration. There were several FRET dye pairs used. FITC and TRITC, AF-647 and Texas Red, AMCA and FITC, and AF-750 and DDAO-S were some of those FRET pairs used. However the main objective was to detect in the IR range, therefore AF-680 and AF-750 were chosen for use as FRET pair. When the donor and the acceptor were labeled with AF-680 and AF-750 respectively, changes in the signal detected were affected by the type of protein used.

There were two techniques chosen for optical detecting of glucose concentration, competitive binding technique and conformational change of a protein.

The competitive binding technique was applied to the GOx, GDH, and Con (A). Dextran (donor) was used as an inhibitor to bind with each of the GOx, GDH, and Con (A) (acceptors). When the labeled dextran binds with the labeled protein and the glucose is introduced to the solution, the glucose will displace dextran due to the high affinity of the enzyme and protein to glucose. This displacement will affect the energy transfer between the donor and acceptor.

There were different enzymes and proteins used in detecting glucose such as GOx, GDH, Con (A), and GBP. Each of the above has different affinities for glucose and also produce different byproducts. GOx was good in detecting glucose but the production of the H_2O_2 provided difficulties for detecting a change in signal after encapsulating in RBCs. Another problem was the weak binding affinity of the dextran to the GOx. This was also a problem with GDH. On the other hand, Con (A) was good protein to use in the competitive binding with dextran. This protein was also used to conduct a study on the effect of the dextran molecular weight on glucose response. The only problem with using Con (A) was the toxicity that will present itself when it is encapsulated in RBCs. It will cause the RBCs to clump during the encapsulation of the nanobiosensor in RBCs. The last protein used was GBP.

GBP provides a hinge type motion due to the conformational change when glucose is present. This motion will be used in detecting glucose by applying FRET. A cysteine site was expressed on GBP and was labeled with a fluorophore (acceptor). The other amino sites were labeled with another fluorophore (donor). When different glucose concentrations were added, a change in FRET took place due to the conformational change. The detection limit was between 0 to 60 μM .

After the development of the glucose nanobiosensor, the encapsulation of RBCs with those nanoprobe was conducted. The RBCs provided shield and protection to nanobiosensors from other proteins and white blood cells. In addition to that, RBCs worked as transporters for glucose, which allowed glucose to enter and exit the RBCs. The optical nanobiosensor was encapsulated in RBCs by using

the Hypo-Osmotic technique. There was a measurable change in signal as the glucose concentration increased.

The detection of signals through porcine tissue such as the skin and aorta was also conducted. The objective was to detect glucose changes from the encapsulated RBCs, but skin is a barrier through which a signal has to be detected. There was different tissue thicknesses used for detection. The range was from 1.41mm to 3.8 mm. A detectable signal was best when the thinnest tissue was used.

Future work will include finding a better NIR FRET pair that has a better quantum yield, a larger area overlap, a larger stokes shift, and remains non-toxic. Several fluorophore vendors such as Molecular Probes and Sigma show increasing advancement in developing more IR dyes. By selecting and testing different FRET dye pairs, it could provide better in vivo detectable signals.

GBP provided good results for detecting glucose, but the detection range needs to be improved. There is a need for more study on the effect of the cysteine site position when it is labeled with one of the fluorophores. Also, further studies are needed on providing several cysteine sites on GBP and how it will affect the glucose response. Different literatures show different results when the cysteine site is at a different position. In this project, the cysteine site was at position 175.

There is a need to develop a better flow system to mimic blood flow in the capillary. Ocean optics will be a highly sensitive tool for detecting signal from the loaded RBCs and also for detecting glucose response.

The long-term effect on the physiology of the encapsulated RBCs is a very important area to study. It appears that the morphology of the loaded cell maintained its shape. In Vivo study will be required to look at any effect on the morphology, as well as the lifetime of the loaded cell.

In conclusion, the development of an optical nanobiosensor for detecting glucose has been achieved. FRET technique is a very simple ratio metric technique that will make the determination of blood glucose concentration change easy to identify. By encapsulating those glucose nanobiosensors in RBCs, those glucose nanobiosensors will be protected from any immune response, which could cause biofouling to the nanobiosensors. The obtained results will be a good foundation for the development of the implantable system for continuous monitoring of blood glucose concentrations optically from outside the body. This system will be minimally invasive during the implantable step and could last for the lifetime of RBCs. This technology will come as a relief to all diabetics who receive treatment from the painful electrochemical system.

REFERENCES

1. Catterall, R.W.; Chemical Sensors. Oxford University Press, Oxford, UK, 1997.
2. Lakowicz, J.R.; Principles of fluorescence spectroscopy. Kluwer Academic/Plenum Publisher, New York, 1999.
3. http://www.pci.tubs.de/aggericke/PC4/Kap_1/jablonsk.htm (4-13-2007).
4. Alvarez-Icaza, M. and Bilitewski, U.; Mass production of biosensors. Anal. Chem. 65:525A-533A, 1993.
5. Wilson, R. and Turner, A.P.F.; Glucose oxidase: an ideal enzyme. Biosensors and Bioelectronics. 7:165-170, 1992.
6. Takahashi, K., Casey, J.L. and Sturtevant, J.M.; Thermodynamic of the binding of d-glucose to yeast hexokinase. Biochemistry. 20:4693-4697, 1981.
7. McShane, M.J.; Potential for glucose monitoring with nanoengineered fluorescent biosensors. Diabetes Technol. Ther. 4:533-538, 2002.
8. Strano, M.S.; The role of surfactant adsorption during ultrasonication in the dispersion of single-walled carbon nanotubes. J. Nanosci. Nanotechnol. 3:81-86, 2003.
9. <http://elchem.kaist.ac.kr/vt/chem-ed/optics/detector/pmt.htmX> (4-13-2007)
10. Claremont, D.J., Sambrook, I.E., Penton, C. and Pickup, J.C.; Subcutaneous implantation of a ferrocene-mediated glucose sensor in pigs. Diabetologia. 29:817-821, 1986.

11. Wisniewski, N., Moussy, F. and Reichert, W.M.; Characterization of implantable biosensor membrane biofouling. *Fresenius Journal of Analytical Chemistry*. 366:611-621, 2000.
12. Pickup, J.C., Shaw, G.W. and Claremont, D.J.; In vivo molecular sensing in diabetes mellitus: an implantable glucose sensor with direct electron transfer. *Diabetologia*. 32:213-217, 1989.
13. Heise, H.M., Marbach, R., Koschinsky, T.H. and Gries, F.A.; Noninvasive blood glucose sensors based on near-infrared spectroscopy. *Artif Organs*. 18:439-447, 1994
14. Robinson, M.R., Eaton, R.P., Haaland, D.M., Koepp, G.W., Thomas, E.V., Stallard, B.R. and Robinson, P.L.; Noninvasive glucose monitoring in diabetic patients a preliminary evaluation. *Clin. Chem*. 38:1618-1622, 1992.
15. Burmeister, J.J., Chung, H., and Arnold, M.A.; Phantoms for noninvasive blood glucose sensing with near infrared transmission spectroscopy. *Photochem. Photobiol*. 67:50–55, 1998.
16. Wang, J.; Bismuth-coated screen-printed electrodes for stripping voltammetric measurements of trace lead. *Electroanalysis*. 13:983-987, 2001.
17. March, W.F., Rabinovitch, B., Adams, R., Wise, J.R., and Melton, M.; Ocular glucose sensor. *Trans. Am. Soc. Artif. Intern. Organ*. 28:232-235, 1982.

18. Rabinovitch, B., March, W.F., and Adams, R.L.; Noninvasive glucose monitoring of the aqueous humor of the eye. Part I. Measurement of very small optical rotations. *Diabetes Care*. 5:254-258, 1982.
19. Shultz, J.S., Mansouri, S., and Goldstein, I.J.; Affinity sensor: a new technique for developing implantable sensors for glucose and other metabolites *Diabetes Care*. 5:245-253, 1982.
20. Quinn, C.P., Pathak, C.P., Heller, A. and Hubbell, J.A.; Photo-crosslinked copolymers of 2-hydroxyethyl methacrylate, poly(ethylene glycol) tetraacrylate and ethylene dimethacrylate for improving biocompatibility of biosensors *Biomaterials*. 16:389-396, 1995.
21. Xu, H., Aylott, J.W., Kopelman, R., Miller, T.J. and Philbert, M.A.; A real-time ratiometric method for the determination of molecular oxygen inside living cells using sol-gel-based spherical optical nanosensors with applications to rat C6 glioma. *Anal. Chem*. 73:4124-4133, 2001.
22. Clark, H.A., Hoyer, M., Philbert, M.A. and Kopelman, R.; Optical nanosensors for chemical analysis inside single living cells. 1. Fabrication, characterization and methods for intracellular delivery of PEBBLE sensors. *Anal. Chem*. 71:4831-4836, 1999.
23. Brasuel, M., Kopelman, R., Miller, T.J., Tjalkens, R. and Philbert, M.A.; Ion-detecting sensors comprising plasticizer-free copolymers. *Anal. Chem*. 73:2221-2228, 2001.
24. Xu, H., Aylott, J.W. and Kopelman, R.; Fluorescent nano-PEBBLE sensors designed for intracellular glucose imaging. *Analyst*. 127:1471-1477, 2002.

25. Ihler, G.M., Glew, R.H. and Schnure, F.W.; Enzyme loading of erythrocytes. *Proc. Natl. Acad. Sci. USA.* 70:2663-2666, 1973.
26. Sprandel, U., Hubbard, A.R. and Chalmers, R.A.; In vitro studies on resealed erythrocyte ghosts as protein carriers. *Res. Exp. Med. (Berlin)* 175:239-245, 1979.
27. Gould, G.W. and Holman, G.D.; The glucose transporter family: structure, function and tissue-specific expression. *Biochem. J.* 295:329-341, 1993.
28. Chalmers, R.A., Sprandel, U. and Hubbard, A.R.; Characteristics in vitro and survival in vivo of erythrocyte 'ghosts' prepared under iso-osmotic conditions by using high voltage electric fields. *Clin. Sci.* 60:2, 1981.
29. <http://www.diabetes.org/home.jsp> (4-13-2007).
30. Selvin, P.R.; Fluorescence resonance energy transfer. *Methods Enzymol.* 246:300-334, 1995.
31. Stryer, L. and Haugland, R.P.; Energy transfer: a spectroscopic ruler. *Proc Natl Acad Sci USA.* 58:719-726, 1967.
32. Berney, C. and Danuser, G.; FRET or No FRET: A Quantitative Comparison. *Biophys J.* 84:3992-4010, 2003.
33. Boyde, A., Wolfe, L.A., Maly, M., and Jones, S.J.; Vital confocal microscopy in bone. *Scanning.* 17:72-85, 1995.
34. Wu, P. and Brand, L.; Resonance energy transfer: methods and applications. *Anal Biochem.* 218:1-13, 1994.

35. Kenworthy, A.K.; Imaging protein-protein interactions using fluorescence resonance energy transfer microscopy. *Methods Enzymol.* 24:289-296, 2001.
36. Gordon, G.W., Berry, G., Liang, X.H., Levine, B. and Herman, B.; Quantitative fluorescence resonance energy transfer measurements using fluorescence microscopy. *Biophys J.* 74:2702-2713, 1998.
37. Diamandis, E.P. and Christopoulos, T.K.; The biotin-(strept)avidin system: principles and applications in biotechnology. *Clin. Chem.* 37:625-636, 1991.
38. Heitzmann, H. and Richards, F.M.; Use of the avidin-biotin complex for specific staining of biological membranes in electron microscopy. *Proc Natl Acad Sci USA.* 71:3537-3541, 1974.
39. Becker, J.M. and Wilchek, M.; Inactivation by avidin of biotin-modified bacteriophage. *Biochim Biophys Acta.* 264:165-170, 1972.
40. Wilchek, M.; Avidin-Biotin Technology. *Methods Enzymol.* 184:10, 1990.
41. Wilchek, M. and Bayer, E.A.; The avidin-biotin complex in bioanalytical applications. *Anal Biochem.* 171:1-32, 1988.
42. Alon, R., Bayer, E.A. and Wilchek, M.; Streptavidin contains an RYD sequence which mimics the RGD receptor domain of fibronectin. *Biochem Biophys Res Commun.* 170:1236-1241, 1991.
43. <http://www2.venus.co.uk/PMDG/AVIDIN.jpg> (4-13-2007)
44. Piran, U. and Riordan, W.J.; Dissociation rate constant of the biotin-streptavidin complex. *J Immunol Methods.* 133:141-143, 1990.

45. http://mgl.scripps.edu/people/gmm/images/btn_1stp.gif (4-13-2007)
46. <http://probes.invitrogen.com/servlets/spectra?fileid=21037p72> (4-13-2007)
47. <http://probes.invitrogen.com/servlets/spectra?fileid=21057p72> (4-13-2007)
48. Arond, L.H. and Frank, H.P.; Molecular weight, molecular weight distribution and molecular size of native dextran. J. Phys. Chem. 58:953, 1954.
49. Elias, H.G.; Die viscosimetrische Molekulargewichtsbestimmung von Polymeren. Makromol. Chem. 33:166, 1959.
50. Antonini, E.; Studies on dextran and dextran derivatives. I. Properties of native dextran in different solvents. Biopolymers. 2:27, 1964.
51. Lindberg, B. and Svensson, S.; Studied the length of. branches in dextran by catalytic oxidation. Acta. Chem. Scand. 22:1907, 1968.
52. Senti, R.F.; Enzymes for carbohydrate analysis and digestion J. Polym. Sci. 17:527, 1955.
53. Granath, K.A.; Measurement of forces between lecithin bilayers. J. Colloid Sci. 13:308, 1958.
54. Wales, M.; Dextran. J. Polym. Sci. 66:101, 1979.
55. Gekko, K.; The delayed basolateral membrane hyperpolarization of the bovine retinal pigment epithelium: mechanism of generation. Am. Chem. Soc. Symposium Series. 150:415, 1981.
56. Arfors, K.E. and Rutili, G.; Gastrointestinal Mucosal Protective Mechanisms. Microvasc. Res. 4:466, 1972.

57. Arfors, K.E. and Rutili, G.; Abstracts.VII Conference on Microcirculation. Aberdeen. 3, 1972.
58. Rutili, G. and Arfors, K.E.; Abstract. Nordic Microcirculation Group Meeting. Ustaoset. 1973.
59. Rutili, G. and Arfors, K.E., Abstracts.VII Conference on Microcirculation. Aberdeen. 101, 1972.
60. Agrawal, B., Goldstein, I., Hassing, G., and So, L.; Protein-Carbohydrate Interaction. VIII. The Preparation and Properties of Acetylated Concanavalin A, the Hemagglutinin of the Jack Bean. Biochem. 7:4211, 1968.
61. Allan, D., Auger, J., and Crumpton, M.; Purification of Concanavalin A receptor from pig lymphocyte plasma membrane. Biochem J. 126:6, 1972.
62. Ambrosino, R., Barone, G., Castronuovo, G., Ceccarini, C., Cultrera, O., and Elia, V.; Protein-Ligand Interaction. A Calorimetric study of the interaction of oligosaccharides and hen ovalbumin glycopeptides with Concanavalin A. Biochem. 26:3971, 1987.
63. Smith, E., and Goldstein, I.; Protein-Carbohydrate Interaction. V. Further inhibition studies directed toward defining the stereochemical requirements of the reactive sites of Concanavalin A. Arch Biochem Biophys. 121:88, 1967.
64. Wang, J.; Bismuth-coated screen-printed electrodes for stripping voltammetric measurements of trace lead Eelectroanalysis. 13:983-987, 2001.

65. Grant, P.S., McShane, M.J.; Development of multilayer fluorescent thin film chemical sensors using electrostatic self assembly. *IEEE Sensors Journal*. 3:139-146, 2003.
66. Birch, D.J.S., Rolinski, O.; Fluorescence Spectroscopy in Biology Advanced Methods and their Applications to Membranes, Proteins, DNA, and Cells. *Res. Chem. Intermed.* 27:425, 2001.
67. Wilson, D.B., and Smith, J.B.; Energy coupling to ATP synthesis by the proton-translocating ATPase. *Bacterial Transport*. 67:495-557, 1978.
68. Furlong, C.E.; *Escherichia coli* and *Salmonella typhimurium*: Cellular and Molecular Biology. *Am. Soc. Microbiol.* 133:768-796, 1987.
69. Ames, G.F.; Bacterial periplasmic transport systems: Structure, mechanism, and evolution. *Annu. Rev. Biochem.* 55:397-425, 1986.
70. Quiocho, F.A., Meador, W.E. & Pflugrath, J.W.; The structure of D-galactose-binding protein at 4.1 Å resolution looks like L-arabinose-binding protein. *J. Mol. Biol.* 133:181-184, 1979.
71. Gilliland, G.L. and Quiocho, F.A.; Hinge-bending in L-arabinose-binding protein. The "Venus's-flytrap" model. *J. Mol. Biol.* 146:341- 362, 1981.
72. Newcomer, M.E., Miller, D.M. and Quiocho, F.A.; Location of the sugar-binding site of L-arabinose-binding protein. Sugar derivative syntheses, sugar binding specificity, and difference Fourier analyses. *J. Biol Chem.* 254:7529-7533, 1979.

73. Newcomer, M.E., Gilliland, G.L. and Quioco, F.A.; L-Arabinose-binding protein-sugar complex at 2.4 Å resolution. Stereochemistry and evidence for a structural change *J. Biol. Chem.* 256:13213-13217, 1981.
74. Ames, G.F.; Bacterial periplasmic transport systems: Structure, mechanism, and evolution. *Annu. Rev. Biochem.* 55, 397–425, 1986
75. Vyas, N.K., Vyas, M.N., and Quioco, F.A.; Sugar and signal-transducer binding sites of the *Escherichia coli* galactose chemoreceptor protein. *Science*. 242:1290-1295, 1988.
76. <http://talaga.rutgers.edu/people/images/GBP.png> (4-13-2007)
77. Sack, J.S., Saper, M.A. and Quioco, F.A., Periplasmic binding protein structure and function: Refined X-ray structures of the leucine/isoleucine/valine-binding protein and its complex with leucine. *J. Mol. Biol.* 206:171-191, 1989.
78. Mahoney, W.C., Hogg, R.W. and Hermodson, M.A.; The amino acid sequence of the D-galactose-binding protein from *Escherichia coli*. *J. Biol. Chem.* 256:4350-4356, 1981.
79. Vyas, N.K., Vyas, M.N. and Quioco, F.A.; Comparison of the periplasmic receptors for L-arabinose, D-glucose/D-galactose, and D-ribose. *J. Biol. Chem.* 266:5226-5237, 1991.
80. Miller, D.M., Olson, J.S., Pflugrath, J.W. and Quioco, F.A.; Rates of ligand binding to periplasmic proteins involved in bacterial transport and chemotaxis. *J. Biol. Chem.* 258:13665-13672, 1983.

81. Deloach J.R.; Carrier and Bioreactor Red Blood Cells for Drug Delivery and Targeting. 326:239–245, 1994.
82. www.people.virginia.edu/~zs9q/zsfig/cell1.jpg (4-13-2007)
83. Magnani M., DeLoach J.R.; the Use of Resealed Erythrocytes as Carriers and Bioreactors. Plenum. 8:53-68, 1992.
84. Hoffman, J.F.; the Use of Resealed Erythrocytes as Carriers and Bioreactors. Plenum. 8:1-15, 1992.
85. Sprandel, U. and Way, J.L.; Erythrocytes as Drug Carriers in Medicine. Plenum. 85:3145-3149, 1997.
86. Green, R. and Widder, K. J.; Drug and Enzyme Targeting. Methods Enzymol. 149:221-312, 1987.
87. Ropars, C., Teisseire, B., Avenard, M., Chassaigne, M., Hurel, C., Girot, R. and Nicolau, C.; Improved oxygen delivery to tissues and iron chelator transport through the use of lysed and resealed red blood cells: a new perspective on Cooley's anemia therapy. Ann. N. Y. Acad. Sci. 445:304-315, 1984.
88. De Flora, A., Zocchi, E., Guida, L., Polvani, C. and Benatti, U.; Conversion of Encapsulated 5-fluoro-2'-deoxyuridine 5'-monophosphate to the Antineoplastic Drug 5-fluoro-2'-deoxyuridine in Human Erythrocytes. Proc. Natl. Acad. Sci. USA. 85:3145-3149, 1988.

89. Rossi, L., Bianchi, M. and Magnani, M.; Increased glucose metabolism by enzyme-loaded erythrocytes in vitro and in vivo normalization of hyperglycemia in diabetic mice. *Biotechnol. Appl. Biochem.* 15: 207-216, 1992.
90. Magnani, M., Giovine, M., Fraternale, A., Damonte, G., Rossi, L., Scarfi' , S., Benatti, U. and De Flora, A.; Erythrocyte-mediated delivery of dexamethasone in patients with chronic obstructive pulmonary disease. *Drug Delivery.* 2:57-61, 1995.
91. Garin, M., Rossi, L., Luque' , S. and Magnani, M.; Band-3 crosslinking-induced targeting of mouse carrier erythrocytes. *Biotechnol. Appl. Biochem.* 22:295-303, 1995.

VITA

Majed El-Dweik was born June 15, 1966, in Alexandria, Egypt. After attending school in Makkah, Saudi Arabia, he received the following degrees; B.S. in Electrical Engineering from the University of Missouri-Columbia, Missouri (1991); M.S. in Electrical Engineering from the University of Missouri-Columbia, Missouri (1992). He joined the family business as a corporate executive for eleven years.

In Fall 2003, he joined the Biological Engineering Department to pursue his Ph.D. degree at the University of Missouri-Columbia. Majed is married to Cathy Dweik of Joplin, Missouri. He is a father of two children, Sarah and Farris.